

1                   ***Manuscript***

2                   **Faster growth rates and higher mortality but similar size-**  
3                   **spectrum in heated, large-scale natural experiment**

4

5       Max Lindmark<sup>a,1</sup>, Malin Karlsson<sup>a</sup>, Anna Gårdmark<sup>b</sup>

6

7       <sup>a</sup> Swedish University of Agricultural Sciences, Department of Aquatic Resources, Institute of  
8       Coastal Research, Skolgatan 6, 742 42 Öregrund, Sweden

9

10      <sup>b</sup> Swedish University of Agricultural Sciences, Department of Aquatic Resources, Box 7018,  
11      750 07 Uppsala, Sweden

12

13      <sup>1</sup> Author to whom correspondence should be addressed. Current address:  
14      Max Lindmark, Swedish University of Agricultural Sciences, Department of Aquatic  
15      Resources, Institute of Marine Research, Turistgatan 5, 453 30 Lysekil, Sweden, Tel.:  
16      +46(0)104784137, email: max.lindmark@slu.se

17

18

19      **Keywords:** body growth, size-structure, size-spectrum, mortality, climate change

20

21

22 Abstract

23 Ectotherms are often predicted to “shrink” with global warming. This is in line with general  
24 growth models and the temperature-size rule (TSR), both predicting smaller adult sizes with  
25 warming. However, they also predict faster juvenile growth rates, leading to larger size-at-age  
26 of young organisms. Hence, the result of warming on the size-structure of a population depends  
27 on the interplay between how mortality rate, juvenile- and adult growth rates are affected by  
28 warming. In this study, we use time series of biological samples spanning more than two  
29 decades from a unique enclosed bay heated by cooling water from a nearby nuclear power plant  
30 to become +8C warmer than its reference area. We used growth-increment biochronologies  
31 (12658 reconstructed length-at-age estimates) to quantify how >20 years of warming has  
32 affected body growth and size-at-age and catch data to quantify mortality rates and population  
33 size-structure of Eurasian perch (*Perca fluviatilis*). In the heated area, growth rates were faster  
34 for all sizes, and hence size-at-age was larger for all ages, compared to the reference area.  
35 However, mortality rates were also higher, such that the difference in the size-spectrum  
36 exponent (describing the proportion of fish by size) was relatively minor and statistically  
37 uncertain. As such, our analysis reveals that mortality, in addition to plastic growth and size-  
38 responses, is a key factor determining the size structure of populations exposed to warming.  
39 Understanding the mechanisms by which warming affects the size-structure of populations is  
40 critical for prediction the impacts of climate change on ecological functions, interactions, and  
41 dynamics.

42

43

44 Significance statement

45 Ecosystem-scale warming experiments provide unique insight into potential impacts of climate  
46 change but are very rare. Our work utilizes an experimental set-up consisting of an enclosed  
47 bay heated by cooling water from a nuclear power plant for more than two decades, and a  
48 reference area. We analyze how changes in growth and mortality have affected the size- and  
49 age distribution in a common freshwater fish using time series of catch data and growth-  
50 increment biochronologies derived from their gill lids. Despite fish in the heated area being  
51 ~10% larger at a given age, elevated mortality rates have resulted in similar size structures.  
52 Accounting for the interplay between mortality and growth is key for predicting climate  
53 impacts on the size-structure of populations.

54

55

56    Introduction

57    Ectotherm species, constituting 99% of species globally (1, 2), are commonly predicted to  
58    shrink in a warming world (3–5). Mean body size responses to temperature may however be  
59    uninformative, as the size-distribution of many species spans several orders of magnitude. For  
60    instance, warming can shift size-distributions without altering mean size if increases in juvenile  
61    size-at-age outweigh the decline in size-at-age in adults, which is consistent with the  
62    temperature size-rule, TSR (6). Resolving how warming induces changes in population size-  
63    distributions may thus be more instructive (7), especially for inferring warming effects on  
64    species' ecological role, biomass production, or energy fluxes (8). This is because key  
65    processes such as metabolism, feeding, growth, mortality scale with body size (9–14). Hence,  
66    as the value of these traits at mean body size is not the same as the mean population trait value  
67    (15), the size-distribution within a population matters for its dynamics and for how it changes  
68    under warming.

69    The population size distribution can be represented as a size-spectrum, which generally is  
70    the frequency distribution of individual body sizes (16). It is often described in terms of the  
71    size-spectrum slope (slope of individuals or biomass of a size class over the mean size of that  
72    class on log-log scale (16–18)) or simply the exponent of the power law individual size-  
73    distribution (16). The size-spectrum thus results from temperature-dependent ecological  
74    processes such as body growth, mortality and recruitment (10, 19). Despite its rich theoretical  
75    foundation (20) and usefulness as an ecological indicator (21), few studies have evaluated  
76    warming-effects on the species size-spectrum in larger bodied species (but see Blanchard *et*  
77    *al.*(21)), and none in large scale experimental set-ups. There are numerous paths by which a  
78    species' size-spectrum could change with warming (19). For instance, in line with TSR  
79    predictions, warming may lead to a smaller size-spectrum exponents (steeper slope) if the  
80    maximum size declines. However, changes in size-at-age and the relative abundances of

81 juveniles and adults may alter this decline in the size-spectrum slope. Warming can also lead  
82 to elevated mortality (12, 22–24), which truncates the age-distribution towards younger  
83 individuals (25). This may reduce density dependence and potentially increase growth rates,  
84 thus countering the effects of mortality on the size spectrum exponent. However, not all sizes  
85 may benefit from warming, as e.g. the optimum temperature for growth declines with size (26).  
86 Hence, the effect of warming on the size-spectrum depends on several interlinked processes  
87 affecting abundance-at-size and size-at-age.

88 Size-at-age is generally predicted to increase with warming for small individuals, but  
89 decrease for large individuals according to the mentioned TSR (6, 27). Several factors likely  
90 contribute to this pattern, such as increased allocation to reproduction (28) and larger  
91 individuals in fish populations having optimum growth rates at lower temperatures (26).  
92 Empirical support in fishes for this pattern seem to be more consistent for increases in size-at-  
93 age of juveniles (29–31) than declines in adult size-at-age (but see (32–34)), for which a larger  
94 diversity in responses is observed among species (e.g., 31, 35). However, most studies have  
95 been done on commercially exploited species (since long time series are more common in such  
96 species), which may confound effects of temperature plastic and/or genetic responses to size-  
97 selective mortality on growth and size-at-age (36).

98 The effect of temperature on mortality rates of wild populations are more studied using  
99 among-species analyses. These relationships based on thermal gradients in space may not  
100 necessarily be the same as the effects of *warming* on mortality on single populations. Hence,  
101 the effects of warming on growth and size-at-age and mortality within natural populations  
102 constitute a key knowledge gap for predicting the consequences of climate change on  
103 population size-spectra.

104 Here we used data from a unique, large-scale 23-year-long heating-experiment of a coastal  
105 ecosystem to quantify how warming changed fish body growth, mortality, and the size structure

106 in an unexploited population of Eurasian perch (*Perca fluviatilis*, ‘perch’). We compare fish  
107 from this enclosed bay exposed to temperatures approximately 8°C above normal (‘heated  
108 area’) with fish from a reference area in the adjacent archipelago (Fig. 1). Using hierarchical  
109 Bayesian models, we quantify differences in key individual- and population level parameters,  
110 such as body growth, asymptotic size, mortality rates, and size-spectra, between the heated and  
111 reference coastal area.

112

## 113 Materials and Methods

### 114 *Data*

115 We use size-at-age data from perch sampled annually from an artificially heated enclosed bay  
116 (‘the Biotest basin’) and its reference area, both in the western Baltic Sea (Fig. 1). Heating  
117 started in 1980, the first analyzed cohort is 1981, and first and last catch year is 1987 and 2003,  
118 respectively, to omit transient dynamics and acute responses, and to ensure we use cohorts that  
119 only experienced one of the thermal environments during its life. A grid at the outlet of the  
120 heated area (Fig. 1) prevented fish larger than 10 cm from migrating between the areas (31,  
121 37), and genetic studies confirm the reproductive isolation between the two populations during  
122 this time-period (38). However, the grid was removed in 2004, and since then fish growing up  
123 in the heated Biotest basin can easily swim out, fish caught in the reference area cannot be  
124 assumed to be born there. Hence, we use data only up until 2003. This resulted in 12658 length-  
125 at-age measurements from 2426 individuals in 256 net deployments.

126 We use data from fishing events using survey-gillnets that took place in October in the  
127 heated Biotest basin and in August in the reference area when temperatures are most  
128 comparable between the two areas (31), because temperature affect catchability in static gears.  
129 The catch was recorded by 2.5 cm length classes during 1987-2000, and into 1 cm length groups  
130 2001-2003. To express lengths in a common length standard, 1 cm intervals were converted

131 into 2.5 cm intervals. The unit of catch data is hence the number of fish caught by 2.5 cm size  
132 class per net per night (i.e., a catch-per-unit-effort [CPUE] variable). All data from fishing  
133 events with disturbance affecting the catch (e.g., seal damage, strong algal growth on the gears,  
134 clogging by drifting algae) were removed (years 1996 and 1999 from the heated area in the  
135 catch data).

136 Length-at-age throughout life was reconstructed for a semi-random length-stratified subset  
137 of caught individuals each year. This was done using growth-increment biochronologies  
138 derived from annuli rings on the operculum bones (with control counts done on otoliths). Such  
139 analyses have become increasingly used to analyze changes in growth and size-at-age of fishes  
140 (39, 40). Specifically, an established power-law relationship between the distance of annual  
141 rings and fish length was used:  $L = \kappa R^s$ , where  $L$  is the length of the fish,  $R$  the operculum  
142 radius,  $\kappa$  the intercept, and  $s$  the slope of the line for the regression of log-fish length on log-  
143 operculum radius from a large reference data set for perch (41). Back-calculated length-at-age  
144 were obtained from the relationship  $L_a = L_s (\frac{r_a}{R})^s$ , where  $L_a$  is the back-calculated body length  
145 at age  $a$ ,  $L_s$  is the final body length (body length at catch),  $r_a$  is the distance from the center to  
146 the annual ring corresponding to age  $a$  and  $s = 0.861$  for perch (41). Since perch exhibits  
147 sexual size-dimorphism, and age-determination together with back calculation of growth was  
148 not done for males in all years, we only used females for our analyses.

149

#### 150 *Statistical Analysis*

151 The differences in size-at-age, growth, mortality, and size structure between perch in the heated  
152 and the reference area were quantified using hierarchical linear and non-linear models fitted in  
153 a Bayesian framework. First, we describe each statistical model and then provide details of  
154 model fitting, model diagnostics and comparison.

155 We fit the von Bertalanffy growth equation (VBGE) (42, 43) on a log scale, describing  
 156 length as a function of age to evaluate differences in size-at-age and asymptotic size:  $\log(L_t) =$   
 157  $\log(L_\infty(1 - e^{(-K(t-t_0))}))$ , where  $L_t$  is the length at age ( $t$ , years),  $L_\infty$  is the asymptotic size,  
 158  $K$  is the Brody growth coefficient ( $yr^{-1}$ ) and  $t_0$  is the age when the average length was zero.  
 159 We used only age- and size-at-catch as the response variables (i.e., not back-calculated length-  
 160 at-age). This was to have a simpler model and not have to account for parameters varying  
 161 within individuals as well as cohorts, as mean sample size per individual was only  $\sim 5$ . We let  
 162 parameters vary among cohorts rather than year of catch, because individuals within cohorts  
 163 share similar environmental conditions and density dependence (39). Eight models in total were  
 164 fitted (with area being dummy-coded), with different combinations of shared and area-specific  
 165 parameters. We evaluated if models with area-specific parameters led to better fit and  
 166 quantified the differences in area-specific parameters (indexed by subscripts heat and ref). The  
 167 model with all area-specific parameter can be written as:

$$168 \quad L_i \sim \text{Student-}t(v, \mu_i, \sigma) \quad (1)$$

$$169 \quad \begin{aligned} \log(\mu_i) &= A_{\text{ref}} \log \left[ L_{\infty \text{ref}j[i]} \left( 1 - e^{(-K_{\text{ref}j[i]}(t - t_{0\text{ref}j[i]}))} \right) \right] + \\ &\quad A_{\text{heat}} \log \left[ L_{\infty \text{heat}j[i]} \left( 1 - e^{(-K_{\text{heat}j[i]}(t - t_{0\text{heat}j[i]}))} \right) \right] \end{aligned} \quad (2)$$

$$170 \quad \begin{bmatrix} L_{\infty \text{ref}j} \\ L_{\infty \text{heat}j} \\ K_{\text{ref}j} \\ K_{\text{heat}j} \end{bmatrix} \sim \text{MVNormal} \left( \begin{bmatrix} \mu_{L_{\infty \text{ref}}} \\ \mu_{L_{\infty \text{heat}}} \\ \mu_{K_{\text{ref}}} \\ \mu_{K_{\text{heat}}} \end{bmatrix}, \begin{bmatrix} \sigma_{L_{\infty \text{ref}}} & 0 & 0 & 0 \\ 0 & \sigma_{L_{\infty \text{heat}}} & 0 & 0 \\ 0 & 0 & \sigma_{K_{\text{ref}}} & 0 \\ 0 & 0 & 0 & \sigma_{K_{\text{heat}}} \end{bmatrix} \right) \quad (3)$$

171 where lengths are *Student-t* distributed to account for extreme observations,  $v$ ,  $\mu$  and  $\phi$   
 172 represent the degrees of freedom, mean and the scale parameter, respectively.  $A_{\text{ref}}$  and  $A_{\text{heat}}$   
 173 are dummy variables such that  $A_{\text{ref}} = 1$  and  $A_{\text{heat}} = 0$  if it is the reference area, and vice versa  
 174 for the heated area. The multivariate normal distribution in Eq. 3 is the prior for the cohort-  
 175 varying parameters  $L_{\infty \text{ref}j}$ ,  $L_{\infty \text{heat}j}$ ,  $K_{\text{ref}j}$  and  $K_{\text{heat}j}$  (for cohorts  $j = 1981, \dots, 1997$ ) (note that  
 176 cohorts extend further back in time than the catch data), with hyper-parameters  $\mu_{L_{\infty \text{ref}}}$ ,  $\mu_{L_{\infty \text{heat}}}$ ,

177  $\mu_{K_{\text{ref}}}, \mu_{K_{\text{heat}}}$  describing the non-varying population means and a covariance matrix with the  
 178 between-cohort variation along the diagonal (note we did not model a correlation between the  
 179 parameters, hence off-diagonals are 0). The other seven models include some or all parameters  
 180 as parameters common for the two areas, e.g., substituting  $L_{\infty\text{ref}j}$  and  $L_{\infty\text{heat}j}$  with  $L_{\infty j}$ . To aid  
 181 convergence of this non-linear model, we used informative priors chosen after visualizing  
 182 draws from prior predictive distributions (44) using probable parameter values (*Supporting*  
 183 *Information*, Fig. S1, S7). We used the same prior distribution for each parameter class for both  
 184 areas to not introduce any other sources of differences in parameter estimates between areas.  
 185 We used the following priors for the VBGE model:  $\mu_{L_{\infty\text{ref,heat}}} \sim N(45, 20)$ ,  
 186  $\mu_{K_{\text{ref,heat}}} \sim N(0.2, 0.1)$ ,  $t_{0\text{ref,heat}} \sim N(-0.5, 1)$  and  $v \sim \text{gamma}(2, 0.1)$ .  $\sigma$  parameters,  $\mu_{L_{\infty\text{ref}}}$ ,  
 187  $\mu_{L_{\infty\text{heat}}}, \mu_{K_{\text{ref}}}, \mu_{K_{\text{heat}}}$  were given a *Student-t*(3, 0, 2.5) prior.

188 We also compared how body growth scales with body size (in contrast to length vs age).  
 189 This is because size-at-age reflects lifetime growth history rather than current growth histories  
 190 and may thus be large because growth was fast early in life, not because current growth rates  
 191 are fast (45). We therefore fit allometric growth models describing how specific growth rate  
 192 scales with length:  $G = \alpha L^\theta$ , where  $G$ , the annual specific growth between year  $t$  and  $t + 1$ , is  
 193 defined as:  $G = 100 \times (\log(L_{t+1}) - \log(L_t))$  and  $L$  is the geometric mean length:  $L =$   
 194  $(L_{t+1} \times L_t)^{0.5}$ . Here we also used back-calculated length-at-age, resulting in multiple  
 195 observations for each individual. As with the VBGE model, we dummy coded area to compare  
 196 models with different combinations of common and shared parameters. We assumed growth  
 197 rates were *Student-t* distributed, and the full model can be written as:

$$L_i \sim \text{Student}-t(v, \mu_i, \sigma) \quad (4)$$

$$\mu_i = A_{\text{ref}}(\alpha_{\text{ref}j[i], k[i]} L^{\theta_{\text{ref}}}) + A_{\text{heat}}(\alpha_{\text{heat}j[i], k[i]} L^{\theta_{\text{heat}}}) \quad (5)$$

$$\alpha_{\text{ref,heat}j} \sim N(\mu_{\alpha_{\text{ref,heat}j}}, \sigma_{\alpha_{\text{ref,heat}j}}) \quad (6)$$

$$\alpha_{\text{ref,heat}j} \sim N(\mu_{\alpha_{\text{ref,heat}j}}, \sigma_{\alpha_{\text{ref,heat}j}}) \quad (7)$$

202  $\theta_{\text{ref},\text{heat}j} \sim N(\mu_{\theta_{\text{ref},\text{heat}j}}, \sigma_{\theta_{\text{ref},\text{heat}j}})$  (8)

203  $\theta_{\text{ref},\text{heat}j} \sim N(\mu_{\theta_{\text{ref},\text{heat}j}}, \sigma_{\theta_{\text{ref},\text{heat}j}})$  (9)

204

205 We assumed only  $\alpha$  varied across individuals  $j$  within cohorts  $k$  and compared two models:  
 206 one with  $\theta$  common for the heated and reference area, and one with an area-specific  $\theta$ . We  
 207 used the following priors, after visual exploration of the prior predictive distribution  
 208 (*Supporting Information*, Fig. S8, S10):  $\alpha_{\text{ref},\text{heat}} \sim N(500, 100)$ ,  $\theta_{\text{ref},\text{heat}} \sim N(-1.2, 0.3)$  and  
 209  $v \sim \text{gamma}(2, 0.1)$ .  $\sigma$ ,  $\sigma_{\text{id:cohort}}$  and  $\sigma_{\text{cohort}}$  were all given a *Student-t* ( $3, 0, 13.3$ ) prior.

210 We estimated total mortality by fitting linear models to the natural log of catch (CPUE) as  
 211 a function of age (catch curve regression), under the assumption that in a closed population,  
 212 the exponential decline can be described as  $N_t = N_0 e^{-Zt}$ , where  $N_t$  is the population at time  $t$ ,  
 213  $N_0$  is the initial population size and  $Z$  is the instantaneous mortality rate. This equation can be  
 214 rewritten as a linear equation:  $\log(C_t) = \log(vN_0) - Zt$ , where  $C_t$  is catch at age  $t$ , if catch  
 215 is assumed proportional to the number of fish (i.e.,  $C_t = vN_t$ ). Hence, the negative of the slope  
 216 of the regression is the mortality rate,  $Z$ . To get catch-at-age data, we constructed area-specific  
 217 age-length keys using the sub-sample of the total (female) catch that was age-determined. Age  
 218 length-keys describe the age-proportions of each length-category (i.e., a matrix with length  
 219 category as rows, ages as columns). Age composition is then estimated for the total catch based  
 220 on the “probability” of fish in each length-category being a certain age. With fit this model  
 221 with and without an  $age \times area$ -interaction, and the former can be written as:

222  $\log(CPUE_i) \sim \text{Student-}t(v, \mu_i, \sigma)$  (10)

223  $\mu_i = \beta_{0j[i]}(\text{area}_{\text{ref}}) + \beta_{1j[i]}(\text{area}_{\text{heat}}) + \beta_{2j[i]}age + \beta_{3j[i]}(age \times \text{area}_{\text{heat}})$  (11)

224 
$$\begin{bmatrix} \beta_{0j} \\ \beta_{1j} \\ \beta_{2j} \\ \beta_{3j} \end{bmatrix} \sim \text{MVNormal} \left( \begin{bmatrix} \mu_{\beta_0} \\ \mu_{\beta_1} \\ \mu_{\beta_2} \\ \mu_{\beta_3} \end{bmatrix}, \begin{bmatrix} \sigma_{\beta_0} & 0 & 0 & 0 \\ 0 & \sigma_{\beta_1} & 0 & 0 \\ 0 & 0 & \sigma_{\beta_2} & 0 \\ 0 & 0 & 0 & \sigma_{\beta_3} \end{bmatrix} \right)$$
 (12)

225

226 where  $\beta_{0j}$  and  $\beta_{1j}$  are the intercepts for the reference and heated areas, respectively,  $\beta_{2j}$  is the  
227 age slope for the reference area and  $\beta_{3j}$  is the interaction between *age* and *area*. All  
228 parameters vary by cohort (for cohort  $j = 1981, \dots, 2000$ ) and their correlation is set to 0 (Eq.  
229 12). We use the following (vague) priors:  $\mu_{\beta_{0,\dots,3j}} \sim N(0, 10)$  (where  $\mu_{\beta_2}$  is the population-level  
230 estimate for  $-Z_{\text{ref}}$  and  $\mu_{\beta_2} + \mu_{\beta_3}$  is the population-level estimate for  $-Z_{\text{heat}}$ ) and  
231  $v \sim \text{gamma}(2, 0.1)$ .  $\sigma$  and  $\sigma_{\beta_{0,\dots,3}}$  were given a *Student-t*(3, 0, 2.5) prior.

232 Lastly, we quantified differences in the size-distributions between the areas using size-  
233 spectrum exponents. We estimate the biomass size-spectrum exponent  $\gamma$  directly, using the  
234 likelihood approach for binned data, i.e., the *MLEbin* method in the R package *sizeSpectra* (16,  
235 46, 47). This method explicitly accounts for uncertainty in body masses *within* size-classes  
236 (bins) in the data and has been shown to be less biased than regression-based methods or the  
237 likelihood method based on bin-midpoints (16, 46). We pooled all years to ensure negative  
238 relationships between biomass and size in the size-classes (as the sign of the relationship varied  
239 between years).

240 All analyses were done using R (48) version 4.0.2 with R Studio (2021.09.1). The packages  
241 within the *tidyverse* (49) collection were used to process and visualize data. Models were  
242 fit using the R package *brms* (50). When priors were not chosen based on the prior predictive  
243 distributions, we used the default priors from *brms* as written above. We used 3 chains and  
244 4000 iterations in total per chain. Models were compared by evaluating their expected  
245 predictive accuracy (expected log pointwise predictive density) using leave-one-out cross-  
246 validation (LOO-CV) (51) while ensuring Pareto  $k$  values  $< 0.7$ , in the R package *loo* (52).  
247 Results of the model comparison can be found in the *Supporting Information*, Table S1-S2. We  
248 used *bayesplot* (53) and *tidybayes* (54) to process and visualize model diagnostics and  
249 posteriors. Model convergence and fit was assessed by ensuring potential scale reduction  
250 factors ( $\hat{R}$ ) were less than 1.1, suggesting all three chains converged to a common distribution)

251 (55), and by visually inspecting trace plots, residuals QQ-plots and with posterior predictive  
252 checks (*Supporting Information*, Fig. S2, S9, S11).

253

## 254 Results

255 Analysis of fish (perch) size-at-age using the von Bertalanffy growth equation (VBGE)  
256 revealed that fish cohorts (year classes) in the heated area both grew faster initially (larger size-  
257 at-age and VBGE  $K$  parameter) and reached larger predicted asymptotic sizes than those in the  
258 unheated reference area (Fig. 2). The model with area-specific VBGE parameters ( $L_\infty$ ,  $K$  and  
259  $t_0$ ) had best out of sample predictive accuracy (the largest expected log pointwise predictive  
260 density for a new observation; Table S1), and there is a clear difference in both the estimated  
261 values for fish asymptotic length ( $L_\infty$ ) and growth rate ( $K$ ) between the heated and reference  
262 area (Fig. 2B-E). For instance, the distribution of differences between the heated and reference  
263 area of the posterior samples for  $L_\infty$  and  $K$  only had 11% and 2%, respectively, of the density  
264 below 0, illustrating that it is likely that the parameters are larger in the heated area (Fig. 2C,  
265 E). We estimated that the asymptotic length of fish in the heated area was 1.16 times larger  
266 than in the reference area ( $L_{\infty\text{heat}} = 45.7[36.8, 56.3]$ ,  $L_{\infty\text{ref}} = 39.4[35.4, 43.9]$ , where the  
267 point estimate is the posterior median and values in brackets correspond to the 95% credible  
268 interval). The growth coefficient was 1.27 times larger in the heated area ( $K_{\text{heat}} =$   
269  $0.19[0.15, 0.23]$ ,  $K_{\text{ref}} = 0.15[0.12, 0.17]$ ). Also  $t_{0\text{heat}}$  was larger than  $t_{0\text{ref}}$   
270 ( $-0.16[-0.21, -0.11]$  vs  $-0.44[-0.56, -0.33]$ , respectively). These differences in growth  
271 parameters lead to fish being approximately 10% larger in the heated area relative to the  
272 reference area (Fig. S4).

273 In addition, we found that growth rates in the reference area were both slower and declined  
274 faster with size compared to the heated area (Fig. 3). The best model for growth ( $G = \alpha L^\theta$ ) had  
275 area-specific  $\alpha$  and  $\theta$  parameters (Table S2). Initial growth ( $\alpha$ ) was estimated to be 1.18 times

276 faster in the heated than in the reference area ( $\alpha_{\text{heat}} = 509.7[460.1, 563.5]$ ,  $\alpha_{\text{ref}} =$   
277  $433.5[413.3, 454.1]$ ), and growth of fish in the heated area decline more slowly with length  
278 than in the reference area ( $\theta_{\text{heat}} = -1.13[-1.16, -1.11]$ ,  $\theta_{\text{ref}} = -1.18[-1.19, -1.16]$ ). The  
279 distribution of differences of the posterior samples for  $\alpha$  and  $\theta$  both only had 0.3% of the  
280 density below 0 (Fig. 3C, E), indicating high probability that length-based growth rates are  
281 faster in the heated area.

282 By analyzing the decline in catch-per-unit-effort over age, we found that the instantaneous  
283 mortality rate  $Z$  (rate at which log abundance declines with age) is higher in the heated area  
284 (Fig. 4). The overlap with zero is 0.05% for the distribution of differences of posterior samples  
285 of  $Z_{\text{heat}}$  and  $Z_{\text{ref}}$  (Fig. 4C). We estimated  $Z_{\text{heat}}$  to be  $0.7[0.67, 0.82]$  and  $Z_{\text{ref}}$  to be  
286  $0.63[0.57, 0.68]$ , which corresponds to annual mortality rates of 53% in the heated area and  
287 47% in the reference area.

288 Lastly, analysis of the size-structure in the two areas revealed that, despite the faster growth  
289 rates and larger sizes in the heated area for fish of all sizes, the higher mortality rates in the  
290 heated area led to largely similar size-structures. Specifically, while largest fish were found in  
291 the heated area, the size-spectrum exponent was only slightly larger in the heated area (Fig.  
292 5A), and their 95% confidence intervals largely overlap (Fig. 5C).

293

## 294 Discussion

295 Our study provides strong evidence for warming-induced differentiation in growth, mortality,  
296 and size-structure in a natural population of an unexploited, temperate fish species exposed to  
297 an ecosystem-scale experiment with 5–10 °C above normal temperatures for more than two  
298 decades. While it is a study on only a single species, these features make it a unique climate  
299 change experiment, as experimental studies on fish to date are much shorter and often on scales  
300 much smaller than whole ecosystems, and long time series of biological samples exist mainly

301 for commercially exploited fish species (29, 32, 34) (in which fisheries exploitation affects  
302 size-structure both directly and indirectly by selecting for fast growing individuals). While  
303 factors other than temperature could have contributed to the observed elevated growth and  
304 mortality, the temperature contrast is unusually large for natural systems (i.e., 5-10 °C, which  
305 can be compared to the 1.35 °C change in the Baltic Sea between 1982 and 2006 (56)).  
306 Moreover, heating occurred at the scale of a whole ecosystem, which makes the findings highly  
307 relevant in the context of global warming.

308 Interestingly, our findings contrast with both broader predictions about declining mean or  
309 adult body sizes based on the GOLT hypothesis (5, 57), and with intraspecific patterns such as  
310 the TSR (temperature-size rule (6)). The contrasts lie in that both asymptotic size and size-at-  
311 age of mature individuals, as well as the proportion of larger individuals were slightly larger  
312 and higher in the heated area—despite the elevated mortality rates. This result was unexpected  
313 for two reasons: optimum growth temperatures generally decline with body size within species  
314 under food satiation in experimental studies (26), and fish tend to mature at smaller body size  
315 and allocate more energy into reproduction as it gets warmer (28). Both patterns have been  
316 used to explain how growth can increase for small and young fish, while large and old fish  
317 typically do not benefit from warming. Our study species is no exception to these rules (31, 58,  
318 59). This suggests that growth dynamics under food satiation may not be directly proportional  
319 to those under natural feeding conditions (60). Moreover, our results suggest that growth  
320 changes emerge not only from direct physiological responses to increased temperatures, but  
321 also from warming-induced changes in the food web, e.g., prey productivity, diet composition  
322 and trophic transfer efficiencies (61). It also highlights that we need to focus on understanding  
323 to what extent the commonly observed increase in size-at-age for juveniles in warm  
324 environments can be maintained as they grow older.

325 Our finding that mortality rates were higher in the heated area was expected—warming  
326 leads to faster metabolic rates, which in turn is associated with shorter life span (11, 62, 63)  
327 (higher “physiological” mortality). Warming may also increase predation mortality, as  
328 predators’ feeding rates increase in order to meet the higher demand of food (12, 14, 23).  
329 However, most evidence to date of the temperature dependence of mortality rates in natural  
330 populations stem from across species studies (12, 13, 64) (but see (23, 24)). Across species  
331 relationships are not necessarily determined by the same processes as within species  
332 relationships; thus, our finding of warming-induced mortality in a heated vs control  
333 environment in two nearby con-specific populations is important.

334 Since a key question for understanding the implications of warming on ectotherm  
335 populations is if larger individuals in a population become rarer or smaller (27, 65), within-  
336 species mortality and growth responses to warming need further study. Importantly, this  
337 requires accounting also for effects of warming on growth, and how responses in growth and  
338 mortality depend on each other. For instance, higher mortality (predation or natural,  
339 physiological mortality) can release intra-specific competition and thus increase growth.  
340 Conversely, altered growth and body sizes can lead to changes in size-specific mortality, such  
341 as predation or starvation. In conclusion, individual-level patterns such as the TSR may be of  
342 limited use for predicting changes on the population-level size structure as it does not concern  
343 changes in abundance-at-size via mortality. Mortality may, however, be an important driver of  
344 the observed shrinking of ectotherms (66). Understanding the mechanisms by which the size-  
345 and age-distribution change with warming is critical for predicting how warming changes  
346 species functions and ecological roles (7, 61, 67). Our findings demonstrate that a key to do  
347 this is to acknowledge temperature effects on both growth and mortality and how they interact.  
348

349 Acknowledgements

350 We thank all staff involved in data collection, and Jens Olsson and Göran Sundblad for  
351 discussion. This study was supported by SLU Quantitative Fish and Fisheries Ecology.

352

### 353 Code and Data Availability

354 All data and R code to reproduce the analyses can be downloaded from a GitHub repository  
355 ([https://github.com/maxlindmark/warm\\_life\\_history](https://github.com/maxlindmark/warm_life_history)) and will be archived on Zenodo upon  
356 publication. Researchers interested in using the data for purposes other than replicating our  
357 analyses are advised to request the data from the authors, as other useful information from the  
358 original data might not be included.

359

### 360 Author Contributions

361 ML conceived the idea and designed the study and the statistical analysis. Data-processing,  
362 initial statistical analyses, and initial writing was done by MK and ML. AG contributed  
363 critically to all mentioned parts of the paper. All authors contributed to the manuscript writing  
364 and gave final approval for publication.

365

### 366 References

- 367 1. E. O. Wilson, *The Diversity of Life* (Harvard University Press, 1992).
- 368 2. D. Atkinson, R. M. Sibly, Why are organisms usually bigger in colder environments?  
369 Making sense of a life history puzzle. *Trends in Ecology & Evolution* **12**, 235–239  
370 (1997).
- 371 3. J. L. Gardner, A. Peters, M. R. Kearney, L. Joseph, R. Heinsohn, Declining body size: a  
372 third universal response to warming? *Trends in Ecology & Evolution* **26**, 285–291  
373 (2011).
- 374 4. J. A. Sheridan, D. Bickford, Shrinking body size as an ecological response to climate  
375 change. *Nature Climate Change* **1**, 401–406 (2011).
- 376 5. W. W. L. Cheung, *et al.*, Shrinking of fishes exacerbates impacts of global ocean changes  
377 on marine ecosystems. *Nature Climate Change* **3**, 254–258 (2013).

- 378 6. D. Atkinson, Temperature and organism size—A biological law for ectotherms?  
379 *Advances in Ecological Research* **25**, 1–58 (1994).
- 380 7. K. J. Fritschie, J. D. Olden, Disentangling the influences of mean body size and size  
381 structure on ecosystem functioning: an example of nutrient recycling by a non-native  
382 crayfish. *Ecology and Evolution* **6**, 159–169 (2016).
- 383 8. G. Yvon-Durocher, J. M. Montoya, M. Trimmer, G. Woodward, Warming alters the size  
384 spectrum and shifts the distribution of biomass in freshwater ecosystems. *Global  
385 Change Biology* **17**, 1681–1694 (2011).
- 386 9. K. H. Andersen, Size-based theory for fisheries advice. *ICES J Mar Sci* **77**, 2445–2455  
387 (2020).
- 388 10. J. L. Blanchard, R. F. Heneghan, J. D. Everett, R. Trebilco, A. J. Richardson, From  
389 bacteria to whales: Using functional size spectra to model marine ecosystems. *Trends in  
390 Ecology & Evolution* **32**, 174–186 (2017).
- 391 11. J. H. Brown, J. F. Gillooly, A. P. Allen, V. M. Savage, G. B. West, Toward a metabolic  
392 theory of ecology. *Ecology* **85**, 1771–1789 (2004).
- 393 12. D. Pauly, On the interrelationships between natural mortality, growth parameters, and  
394 mean environmental temperature in 175 fish stocks. *ICES Journal of Marine Science* **39**,  
395 175–192 (1980).
- 396 13. J. T. Thorson, S. B. Munch, J. M. Cope, J. Gao, Predicting life history parameters for all  
397 fishes worldwide. *Ecological Applications* **27**, 2262–2276 (2017).
- 398 14. E. Ursin, A Mathematical Model of Some Aspects of Fish Growth, Respiration, and  
399 Mortality. *Journal of the Fisheries Research Board of Canada* **24**, 2355–2453 (1967).
- 400 15. J. R. Bernhardt, J. M. Sunday, P. L. Thompson, M. I. O'Connor, Nonlinear averaging of  
401 thermal experience predicts population growth rates in a thermally variable  
402 environment. *Proceedings of the Royal Society B: Biological Sciences* **285**, 20181076  
403 (2018).
- 404 16. A. M. Edwards, J. P. W. Robinson, M. J. Plank, J. K. Baum, J. L. Blanchard, Testing and  
405 recommending methods for fitting size spectra to data. *Methods in Ecology and  
406 Evolution* **8**, 57–67 (2017).
- 407 17. R. W. Sheldon, W. H. Sutcliffe, A. Prakash, The Production of Particles in the Surface  
408 Waters of the Ocean with Particular Reference to the Sargasso Sea1. *Limnology and  
409 Oceanography* **18**, 719–733 (1973).
- 410 18. E. P. White, S. K. M. Ernest, A. J. Kerkhoff, B. J. Enquist, Relationships between body  
411 size and abundance in ecology. *Trends in Ecology & Evolution* **22**, 323–330 (2007).
- 412 19. R. F. Heneghan, I. A. Hatton, E. D. Galbraith, Climate change impacts on marine  
413 ecosystems through the lens of the size spectrum. *Emerging Topics in Life Sciences* **3**,  
414 233–243 (2019).

- 415 20. K. H. Andersen, *Fish Ecology, Evolution, and Exploitation: A New Theoretical Synthesis*  
416 (Princeton University Press, 2019).
- 417 21. J. L. Blanchard, *et al.*, Do climate and fishing influence size-based indicators of Celtic  
418 Sea fish community structure? *ICES Journal of Marine Science* **62**, 405–411 (2005).
- 419 22. H. K. Barnett, T. P. Quinn, M. Bhuthimethee, J. R. Winton, Increased prespawning  
420 mortality threatens an integrated natural- and hatchery-origin sockeye salmon  
421 population in the Lake Washington Basin. *Fisheries Research* **227**, 105527 (2020).
- 422 23. P. A. Biro, J. R. Post, D. J. Booth, Mechanisms for climate-induced mortality of fish  
423 populations in whole-lake experiments. *Proceedings of the National Academy of  
424 Sciences* **104**, 9715–9719 (2007).
- 425 24. T. Berggren, U. Bergström, G. Sundblad, Ö. Östman, Warmer water increases early body  
426 growth of northern pike (*Esox lucius*) but mortality has larger impact on decreasing  
427 body sizes. *Can. J. Fish. Aquat. Sci.* (2021) <https://doi.org/10.1139/cjfas-2020-0386>  
428 (October 27, 2021).
- 429 25. L. A. K. Barnett, T. A. Branch, R. A. Ranasinghe, T. E. Essington, Old-Growth Fishes  
430 Become Scarce under Fishing. *Current Biology* **27**, 2843–2848.e2 (2017).
- 431 26. M. Lindmark, J. Ohlberger, A. Gårdmark, Optimum growth temperature declines with  
432 body size within fish species. *Global Change Biology* **28**, 2259–2271 (2022).
- 433 27. J. Ohlberger, Climate warming and ectotherm body size – from individual physiology to  
434 community ecology. *Functional Ecology* **27**, 991–1001 (2013).
- 435 28. H. F. Wootton, J. R. Morrongiello, T. Schmitt, A. Audzijonyte, Smaller adult fish size in  
436 warmer water is not explained by elevated metabolism. *Ecology Letters* **25**, 1177–1188  
437 (2022).
- 438 29. R. E. Thresher, J. A. Koslow, A. K. Morison, D. C. Smith, Depth-mediated reversal of  
439 the effects of climate change on long-term growth rates of exploited marine fish.  
440 *Proceedings of the National Academy of Sciences, USA* **104**, 7461–7465 (2007).
- 441 30. A. Rindorf, H. Jensen, C. Schrum, Growth, temperature, and density relationships of  
442 North Sea cod (*Gadus morhua*). *Canadian Journal of Fisheries and Aquatic Sciences*  
443 **65**, 456–470 (2008).
- 444 31. M. Huss, M. Lindmark, P. Jacobson, R. M. van Dorst, A. Gårdmark, Experimental  
445 evidence of gradual size-dependent shifts in body size and growth of fish in response to  
446 warming. *Glob Change Biol* **25**, 2285–2295 (2019).
- 447 32. S. Smoliński, *et al.*, Century-long cod otolith biochronology reveals individual growth  
448 plasticity in response to temperature. *Sci Rep* **10**, 16708 (2020).
- 449 33. K. B. Oke, F. J. Mueter, M. A. Litzow, Warming leads to opposite patterns in weight-at-  
450 age for young versus old age classes of Bering Sea walleye pollock. *Can. J. Fish. Aquat.  
451 Sci.* (2022) <https://doi.org/10.1139/cjfas-2021-0315> (July 22, 2022).

- 452 34. A. R. Baudron, C. L. Needle, A. D. Rijnsdorp, C. T. Marshall, Warming temperatures  
453 and smaller body sizes: synchronous changes in growth of North Sea fishes. *Global*  
454 *Change Biology* **20**, 1023–1031 (2014).
- 455 35. D. R. Barneche, M. Jahn, F. Seebacher, Warming increases the cost of growth in a model  
456 vertebrate. *Functional Ecology* **33**, 1256–1266 (2019).
- 457 36. A. Audzijonyte, *et al.*, Trends and management implications of human-influenced life-  
458 history changes in marine ectotherms. *Fish and Fisheries* **17**, 1005–1028 (2016).
- 459 37. A. Adill, K. Mo, A. Sevastik, J. Olsson, L. Bergström, “Biologisk recipientkontroll vid  
460 Forsmarks kärnkraftverk (in Swedish)” (2013) (August 10, 2021).
- 461 38. M. Björklund, T. Aho, J. Behrmann-Godel, Isolation over 35 years in a heated biotest  
462 basin causes selection on MHC class II $\beta$  genes in the European perch (*Perca fluviatilis*  
463 L.). *Ecol Evol* **5**, 1440–1455 (2015).
- 464 39. J. R. Morrongiello, R. E. Thresher, A statistical framework to explore ontogenetic growth  
465 variation among individuals and populations: a marine fish example. *Ecological*  
466 *Monographs* **85**, 93–115 (2015).
- 467 40. T. E. Essington, M. E. Matta, B. A. Black, T. E. Helser, P. D. Spencer, Fitting growth  
468 models to otolith increments to reveal time-varying growth. *Can. J. Fish. Aquat. Sci.* **79**,  
469 159–167 (2022).
- 470 41. G. Thoresson, “Metoder för övervakning av kustfiskbestånd (in Swedish)”  
471 (Kustlaboratoriet, Fiskeriverket, 1996) (September 28, 2021).
- 472 42. R. J. H. Beverton, S. J. Holt, *On the Dynamics of Exploited Fish Populations* (Fishery  
473 Investigations London Series 2, Volume 19., 1957).
- 474 43. L. von Bertalanffy, A quantitative theory of organic growth (inquiries on growth laws.  
475 II). *Human Biology* **10**, 181–213 (1938).
- 476 44. J. S. Wesner, J. P. F. Pomeranz, Choosing priors in Bayesian ecological models by  
477 simulating from the prior predictive distribution. *Ecosphere* **12**, e03739 (2021).
- 478 45. K. Lorenzen, Toward a new paradigm for growth modeling in fisheries stock  
479 assessments: Embracing plasticity and its consequences. *Fisheries Research* **180**, 4–22  
480 (2016).
- 481 46. A. M. Edwards, J. P. W. Robinson, J. L. Blanchard, J. K. Baum, M. J. Plank, Accounting  
482 for the bin structure of data removes bias when fitting size spectra. *Marine Ecology*  
483 *Progress Series* **636**, 19–33 (2020).
- 484 47. A. Edwards, sizeSpectra: Fitting Size Spectra to Ecological Data Using Maximum  
485 Likelihood (2020).
- 486 48. R Core Team, *R: A Language and Environment for Statistical Computing*. R Foundation  
487 for Statistical Computing (2020).

- 488 49. H. Wickham, *et al.*, Welcome to the tidyverse. *Journal of Open Source Software*, 1686  
489 (2019).
- 490 50. P.-C. Bürkner, **brms** : An *R* Package for Bayesian Multilevel Models Using *Stan*. *Journal*  
491 *of Statistical Software* **80** (2017).
- 492 51. A. Vehtari, A. Gelman, J. Gabry, Practical Bayesian model evaluation using leave-one-  
493 out cross-validation and WAIC. *Stat Comput* **27**, 1413–1432 (2017).
- 494 52. A. Vehtari, *et al.*, loo: Efficient leave-one-out cross-validation and WAIC for Bayesian  
495 models. (2020).
- 496 53. J. Gabry, D. Simpson, A. Vehtari, M. Betancourt, A. Gelman, Visualization in Bayesian  
497 workflow. *J. R. Stat. Soc. A* **182**, 389–402 (2019).
- 498 54. M. Kay, tidybayes: Tidy Data and Geoms for Bayesian Models (2019).
- 499 55. A. Gelman, J. Carlin, H. Stern, D. Rubin, *Bayesian Data Analysis. 2nd edition* (Chapman  
500 and Hall/CRC, 2003).
- 501 56. I. M. Belkin, Rapid warming of large marine ecosystems. *Progress in Oceanography* **81**,  
502 207–213 (2009).
- 503 57. D. Pauly, The gill-oxygen limitation theory (GOLT) and its critics. *Science Advances* **7**,  
504 eabc6050 (2021).
- 505 58. P. Karås, G. Thoresson, An application of a bioenergetics model to Eurasian perch (*Perca*  
506 *fluviatilis* L.). *Journal of Fish Biology* **41**, 217–230 (1992).
- 507 59. O. Sandström, E. Neuman, G. Thoresson, Effects of temperature on life history variables  
508 in perch. *Journal of Fish Biology* **47**, 652–670 (1995).
- 509 60. S. F. Railsback, What We Don't Know About the Effects of Temperature on Salmonid  
510 Growth. *Transactions of the American Fisheries Society* **151**, 3–12 (2022).
- 511 61. A. Gårdmark, M. Huss, Individual variation and interactions explain food web responses  
512 to global warming. *Philosophical Transactions of the Royal Society B: Biological*  
513 *Sciences* **375**, 20190449 (2020).
- 514 62. M. W. McCoy, J. F. Gillooly, Predicting natural mortality rates of plants and animals.  
515 *Ecology Letters* **11**, 710–716 (2008).
- 516 63. S. B. Munch, S. Salinas, Latitudinal variation in lifespan within species is explained by  
517 the metabolic theory of ecology. *Proceedings of the National Academy of Sciences* **106**,  
518 13860–13864 (2009).
- 519 64. H. Gislason, N. Daan, J. C. Rice, J. G. Pope, Size, growth, temperature and the natural  
520 mortality of marine fish: Natural mortality and size. *Fish and Fisheries* **11**, 149–158  
521 (2010).
- 522 65. J. Ohlberger, E. J. Ward, D. E. Schindler, B. Lewis, Demographic changes in Chinook  
523 salmon across the Northeast Pacific Ocean. *Fish and Fisheries* **19**, 533–546 (2018).

524 66. I. Peralta-Maraver, E. L. Rezende, Heat tolerance in ectotherms scales predictably with  
525 body size. *Nat. Clim. Chang.* **11**, 58–63 (2021).

526 67. A. Audzijonyte, *et al.*, Fish body sizes change with temperature but not all species shrink  
527 with warming. *Nat Ecol Evol* **4**, 809–814 (2020).

528

529

530

531 Figures



532

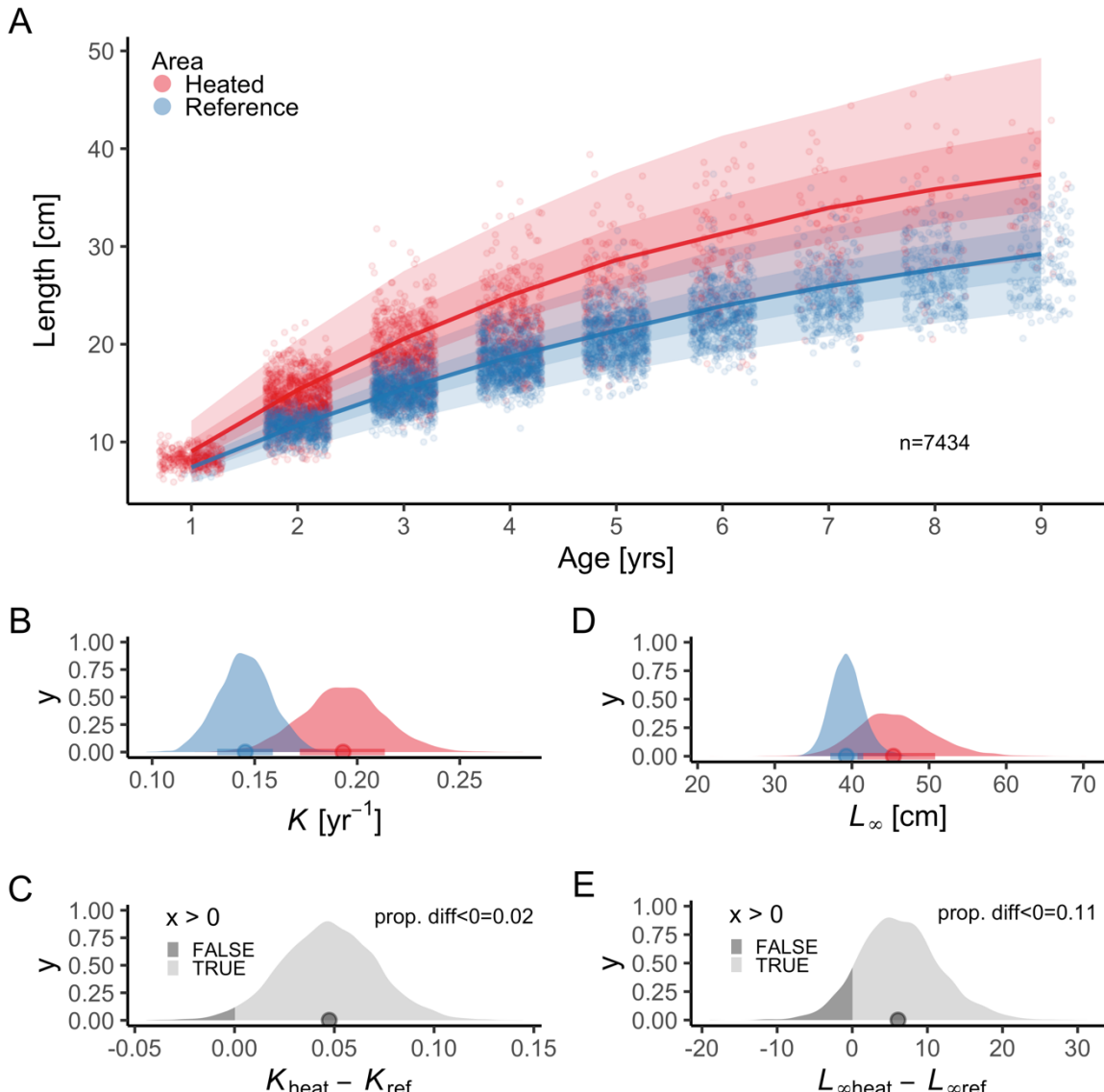
533 **Fig. 1.** Map of the area with the unique whole-ecosystem warming experiment from which  
534 perch in this study was sampled. Inset shows the 1 km<sup>2</sup> enclosed coastal bay that has been  
535 artificially heated for 23 years, the adjacent reference area with natural temperatures, and  
536 locations of the cooling water intake and where the heated water outlet from nuclear power  
537 plants enters the heated coastal basin.

538

539

540

541



542

543 **Fig. 2.** Fish grow faster and reach larger sizes in the heated (red) enclosed bay compared to the  
 544 reference (blue) area. Points in panel (A) depict individual-level length-at-age and lines show  
 545 the global posterior prediction (both exponentiated) without group-level effects (i.e., cohort)  
 546 from the von Bertalanffy growth model with area-specific coefficients. The shaded areas  
 547 correspond to 50% and 90% credible intervals. Panel (B) shows the posterior distributions for  
 548 growth coefficient (parameters  $K_{\text{heat}}$  (red) and  $K_{\text{ref}}$  (blue)) and (C) the distribution of their  
 549 difference. Panel (D) shows the posterior distributions for asymptotic length (parameters  
 550  $L_{\infty\text{heat}}$  and  $L_{\infty\text{ref}}$ ), and (E) the distribution of their difference.

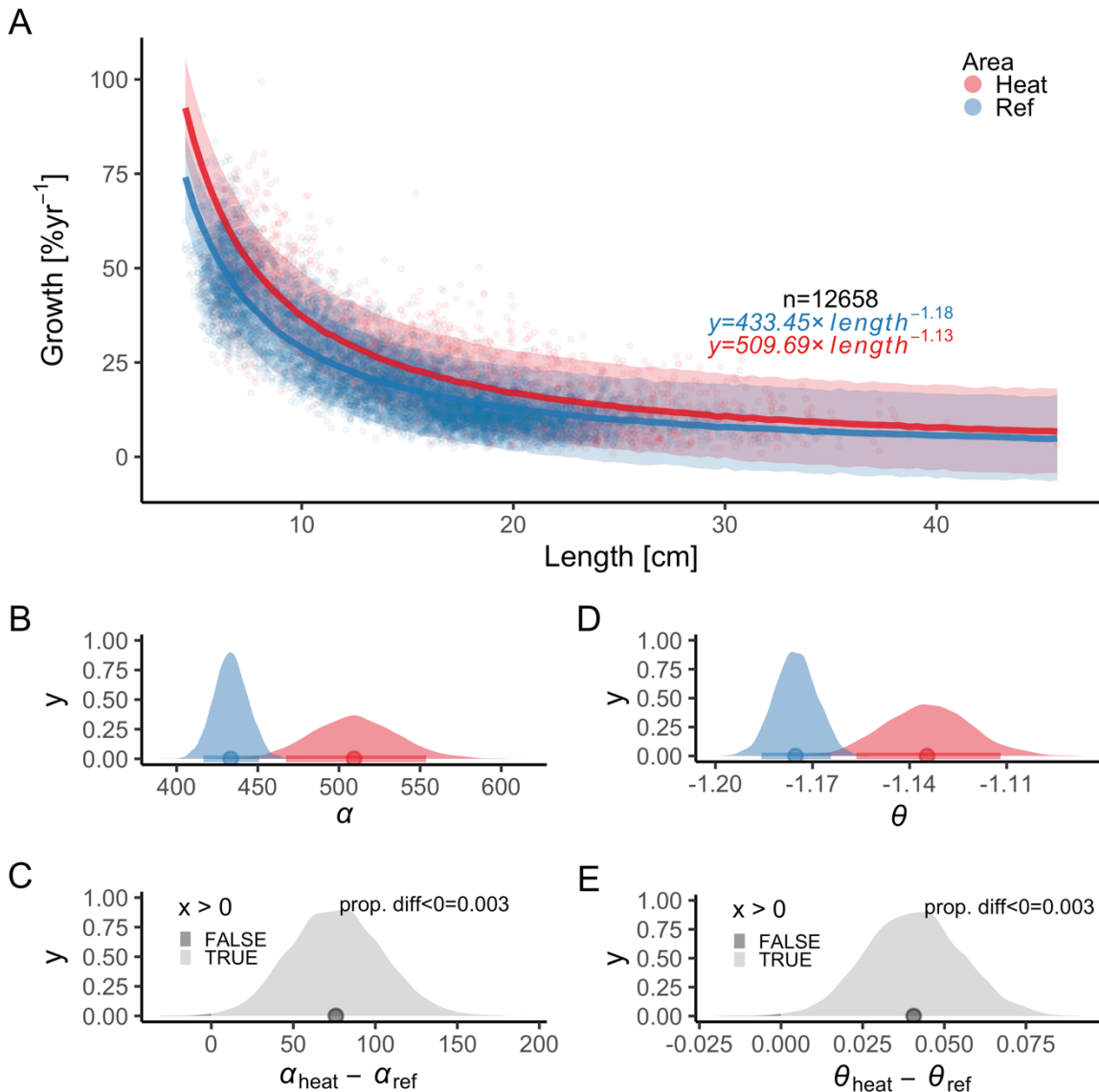
551

552

553

554

555



556

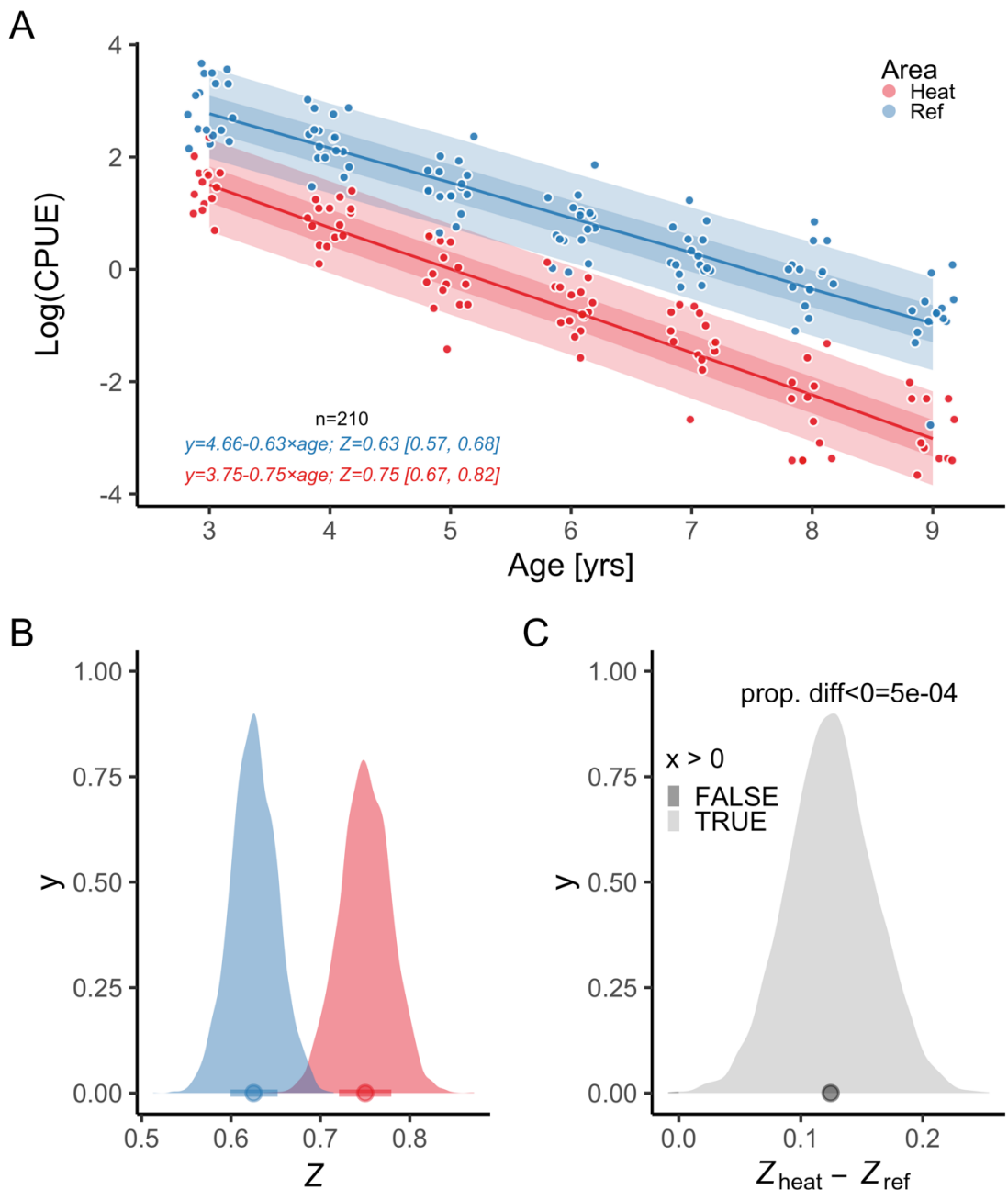
557 **Fig. 3.** The faster growth rates in the heated area (red) compared to the reference (blue) are  
 558 maintained as fish grow. The points illustrate specific growth estimated from back-calculated  
 559 length-at-age (within individuals) as a function of length (expressed as the geometric mean of  
 560 the length at the start and end of the time interval). Lines show the global posterior prediction  
 561 without group-level effects (i.e., individual within cohort) from the allometric growth model  
 562 with area-specific coefficients. The shaded areas correspond to the 90% credible interval. The  
 563 equation uses mean parameter estimates. Panel (B) shows the posterior distributions for initial  
 564 growth ( $\alpha_{\text{heat}}$  (red) and  $\alpha_{\text{ref}}$  (blue)), and (C) the distribution of their difference. Panel (D)  
 565 shows the posterior distributions for the allometric decline in growth with length ( $\theta_{\text{heat}}$  and  
 566  $\theta_{\text{ref}}$ ), and (E) the distribution of their difference.

567

568

569

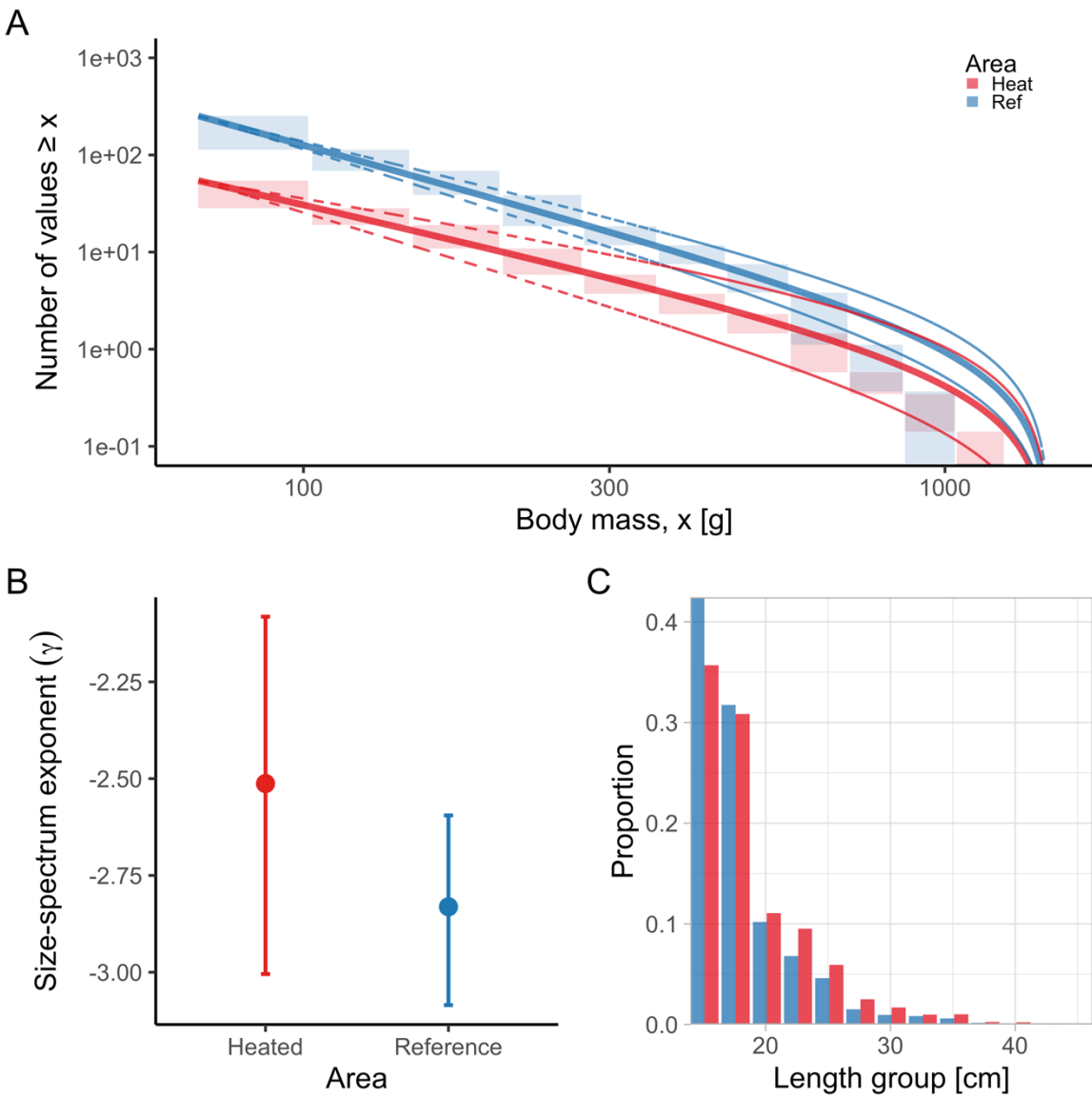
570



571

572 **Fig. 4.** The instantaneous mortality rate ( $Z$ ) is higher in the heated area (red) than in the  
573 reference (blue). Panel (A) shows the  $\log$  (CPUE) as a function of *age*, where the slope  
574 corresponds to the global  $-Z$ . Lines show the posterior prediction without group-level effects  
575 (i.e., cohort) and the shaded areas correspond to the 50% and 90% credible intervals. The  
576 equation uses mean parameter estimates. Panel (B) shows the posterior distributions for  
577 mortality rate ( $Z_{\text{heat}}$  and  $Z_{\text{ref}}$ ), and (C) the distribution of their difference.

578



579

580 **Fig. 5.** The heated area (red) has a larger proportion of large fish than the reference area (blue),  
 581 illustrated both in terms of the biomass size-spectrum (A), and histograms of proportions (C),  
 582 but the difference in the slope of the size-spectra between the areas is not statistically clear (B).  
 583 Panel (A) shows the size distribution and MLEbins fit (red and blue solid curve for the heated  
 584 and reference area, respectively) with 95% confidence intervals indicated by dashed lines. The  
 585 vertical span of rectangles illustrates the possible range of the number of individuals with body  
 586 mass  $\geq$  the body mass of individuals in that bin. Panel (B) shows the estimate of the size-  
 587 spectrum exponent,  $\gamma$ , and vertical lines depict the 95% confidence interval. Panel (C)  
 588 illustrates histograms of length groups in the heated and reference area as proportions (for all  
 589 years pooled).

1                   ***Supporting Information Appendix***

2                   **Faster growth rates and higher mortality but similar size-**  
3                   **spectrum in heated, large-scale natural experiment**

4                   Max Lindmark<sup>a,1</sup>, Malin Karlsson<sup>a</sup>, Anna Gårdmark<sup>b</sup>

5

6                   <sup>a</sup> Swedish University of Agricultural Sciences, Department of Aquatic Resources, Institute of  
7                   Coastal Research, Skolgatan 6, 742 42 Öregrund, Sweden

8                   <sup>b</sup> Swedish University of Agricultural Sciences, Department of Aquatic Resources, Box 7018,  
9                   750 07 Uppsala, Sweden

10

11                 <sup>1</sup> Author to whom correspondence should be addressed. Current address:

12                  Max Lindmark, Swedish University of Agricultural Sciences, Department of Aquatic  
13                  Resources, Institute of Marine Research, Turistgatan 5, 453 30 Lysekil , Sweden, Tel.:  
14                  +46(0)104784137, email: max.lindmark@slu.se

15

16

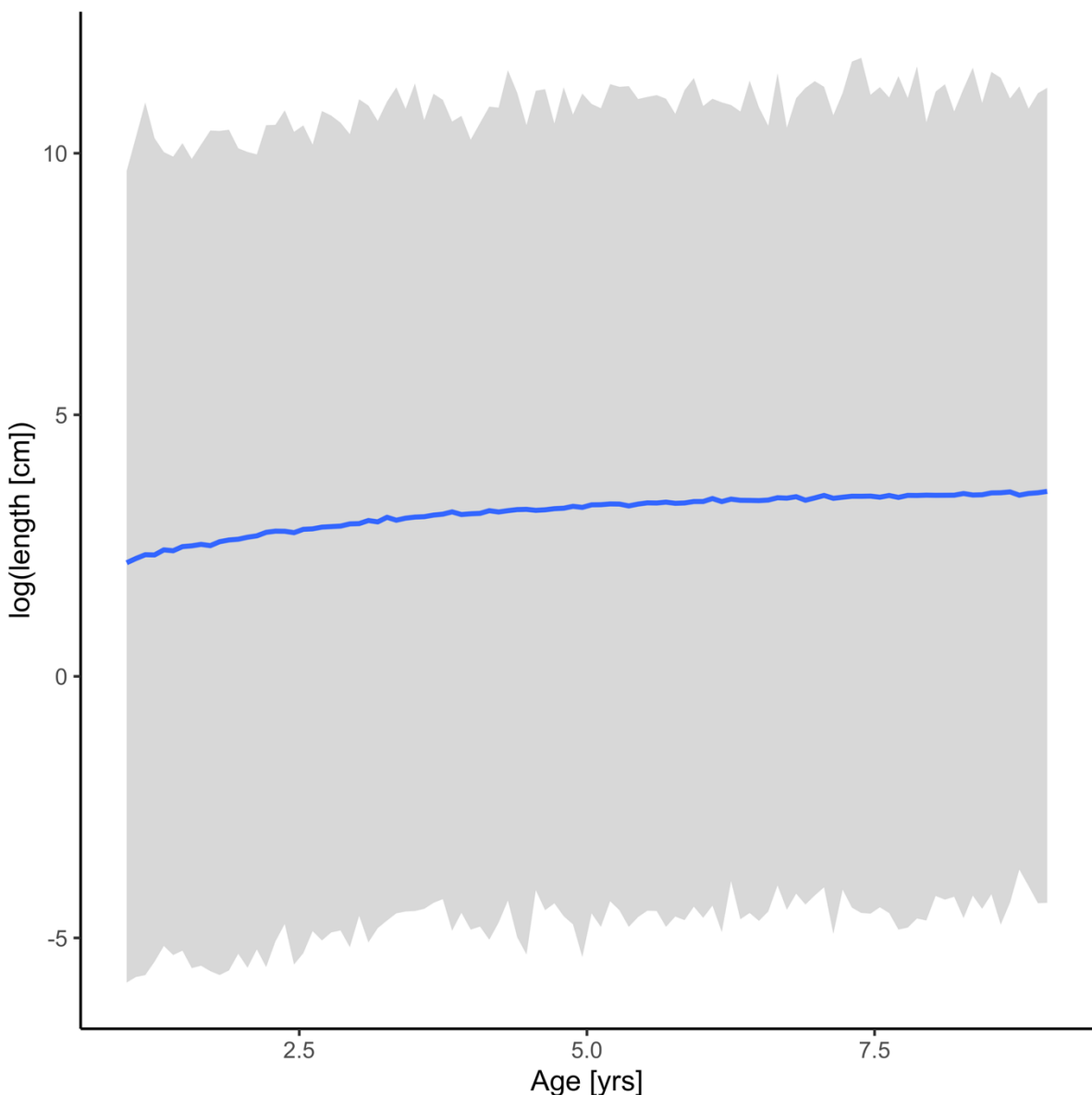
17

18

19

20

21



22

23 **Fig. S1.** Prior predictive distribution for the von Bertalanffy growth equation (posterior draws  
24 from the prior only, ignoring the likelihood). The solid line is the median and the shaded area  
25 is the 95% credible intervals.

26

27

28

29

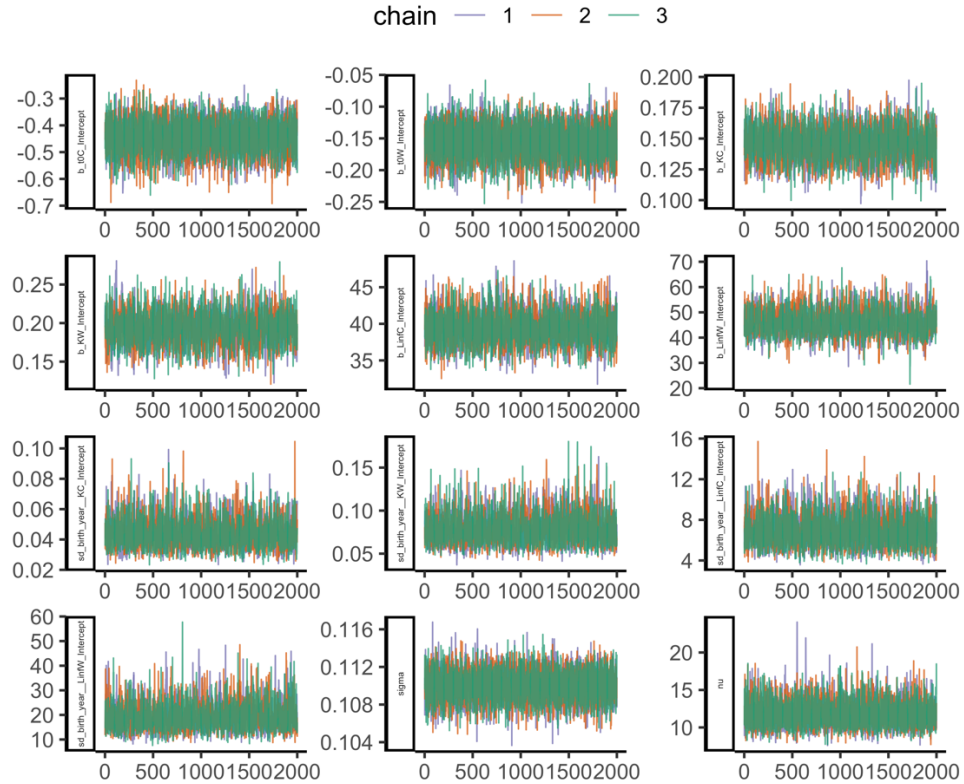
30

31 **Table S1.** Comparison of von Bertalanffy growth models with different combinations of  
 32 shared and area-specific parameters (ordered by difference in expected log pointwise density  
 33 (*elpd*) from the best model). Note that in all models,  $L_{\infty_j}$  and  $K_j$  vary among cohorts.

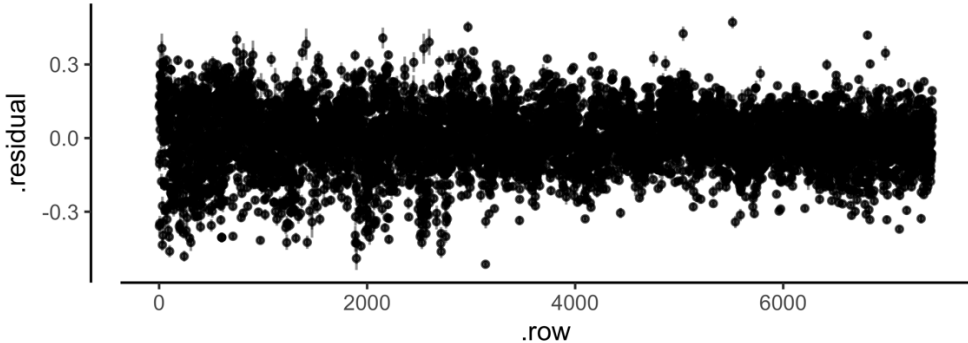
<b>Model Name</b>	<b>Model structure</b>	<b>elpd_diff</b>
M1	Area-specific $L_{\infty_j}$ , $K_j$ and $t_0$	0
M4	Area-specific $L_{\infty_j}$ and $K_j$ , common $t_0$	-9
M2	Area-specific $K_j$ , common $t_0$ and $L_{\infty_j}$	-111
M3	Area-specific $t_0$ and $L_{\infty_j}$ , common $K_j$	-150.5
M7	Area-specific $L_{\infty_j}$ , common $K_j$ and $t_0$	-157.7
M6	Area-specific $K_j$ , common $t_0$ and $L_{\infty_j}$	-173.9
M5	Area-specific $t_0$ , common $K_j$ and $L_{\infty_j}$	-1337.5
M8	Common $t_0$ , $K_j$ and $L_{\infty_j}$	-2153.8

34  
 35  
 36  
 37  
 38  
 39  
 40  
 41  
 42  
 43  
 44

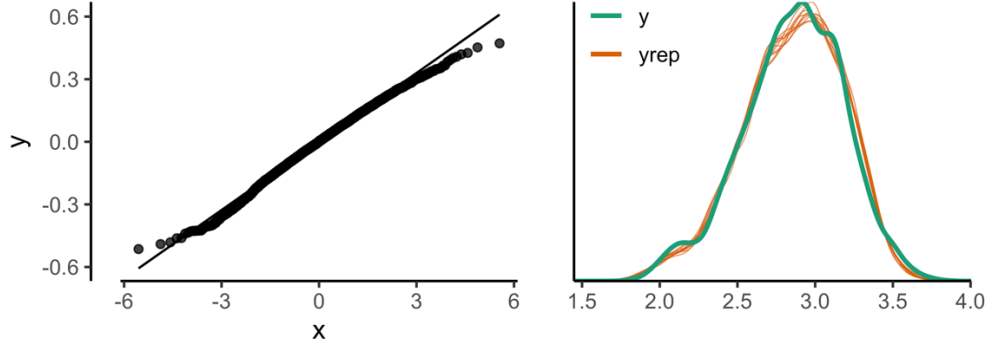
A



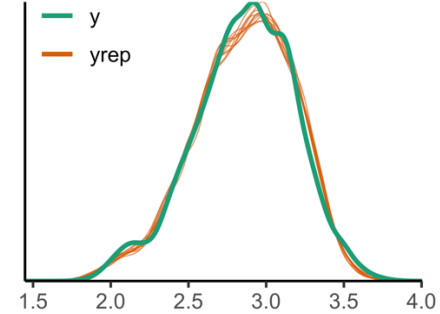
B



C

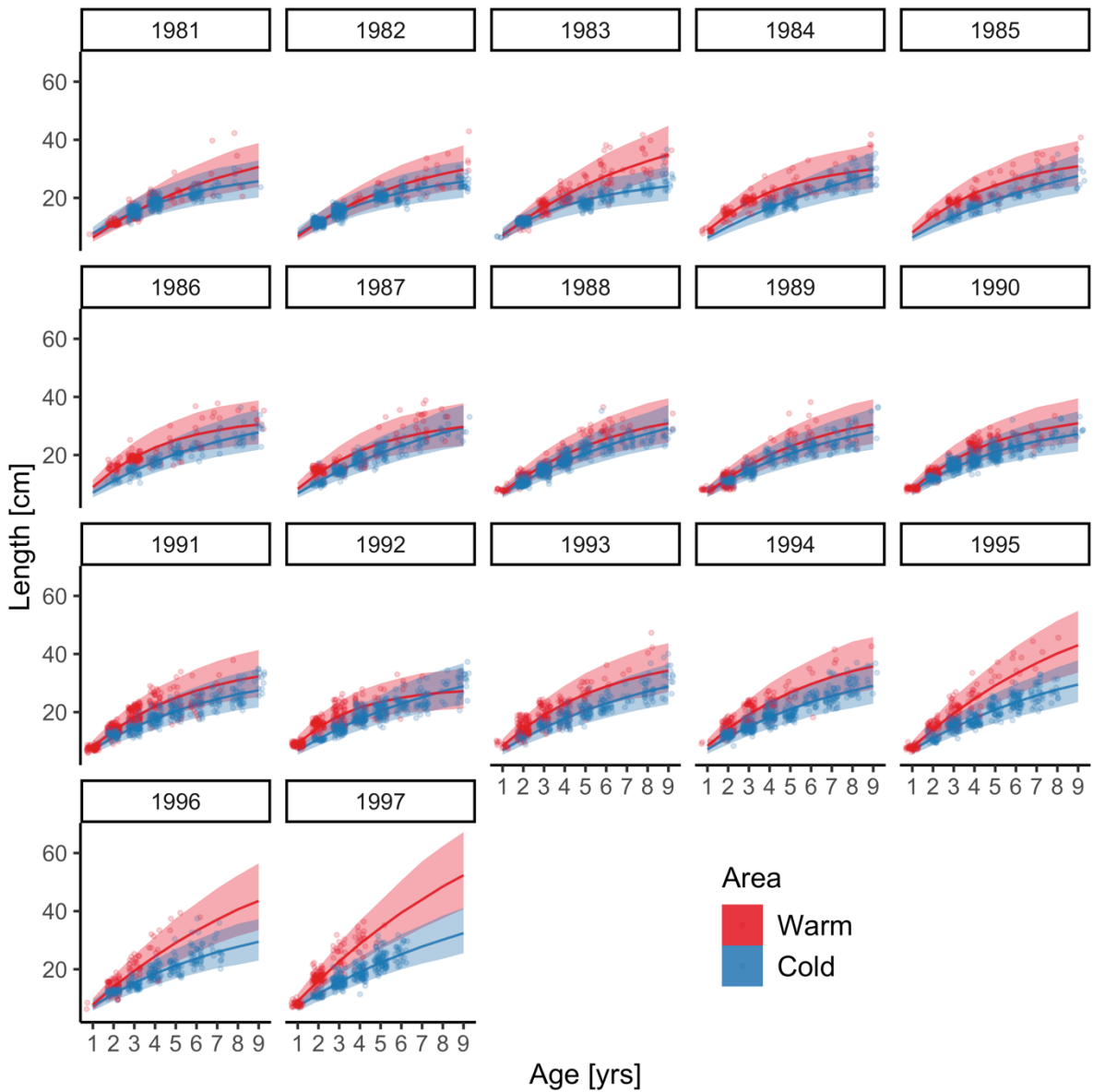


D



45

46 **Fig. S2.** The best model of the von Bertalanffy growth equation: (A) traceplot to illustrate chain  
 47 convergence for key (population-level) parameters, (B) residuals, (C) QQ-plot and (D)  
 48 posterior predictive check (D).



49

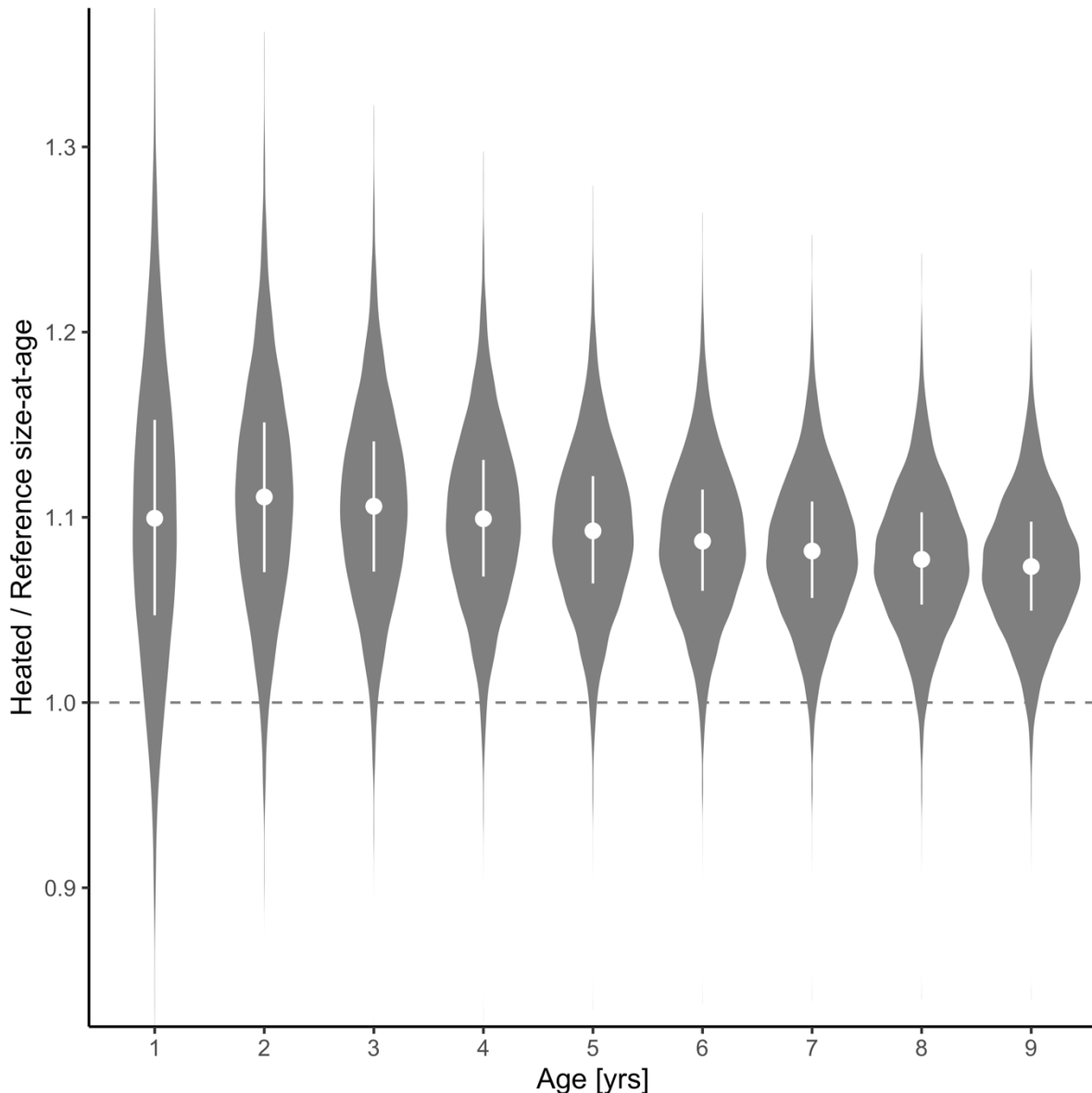
50 **Fig. S3.** Cohort-specific predictions from the best von Bertalanffy model (i.e., with cohort-  
 51 varying  $L_\infty$  and  $K$ ). Points correspond to data; solid lines correspond to the median of the  
 52 posterior prediction from the model and the shaded area corresponds to the 95% credible  
 53 interval.

54

55

56

57



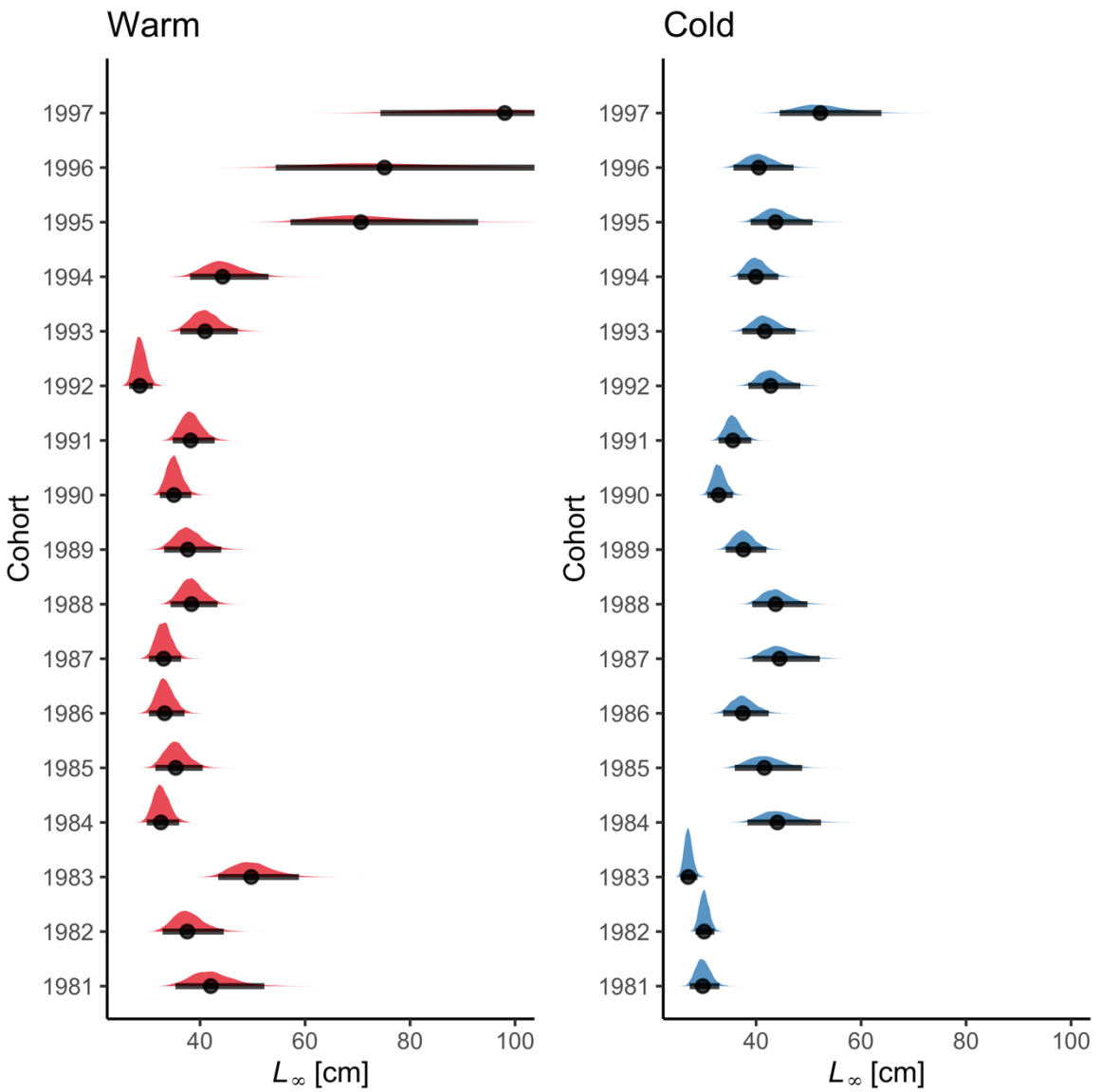
58

59 **Fig. S4.** The average length-at-age is larger for fish of all ages in the heated enclosed bay  
 60 compared to the reference area, and the relative difference declines very slightly with age.  
 61 Violin plots depict size-at-age in the heated relative to the reference area, based on draws from  
 62 expectation of the posterior predictive distribution (without random effects). The points and  
 63 vertical lines depict the median and the interquartile range.

64

65

66

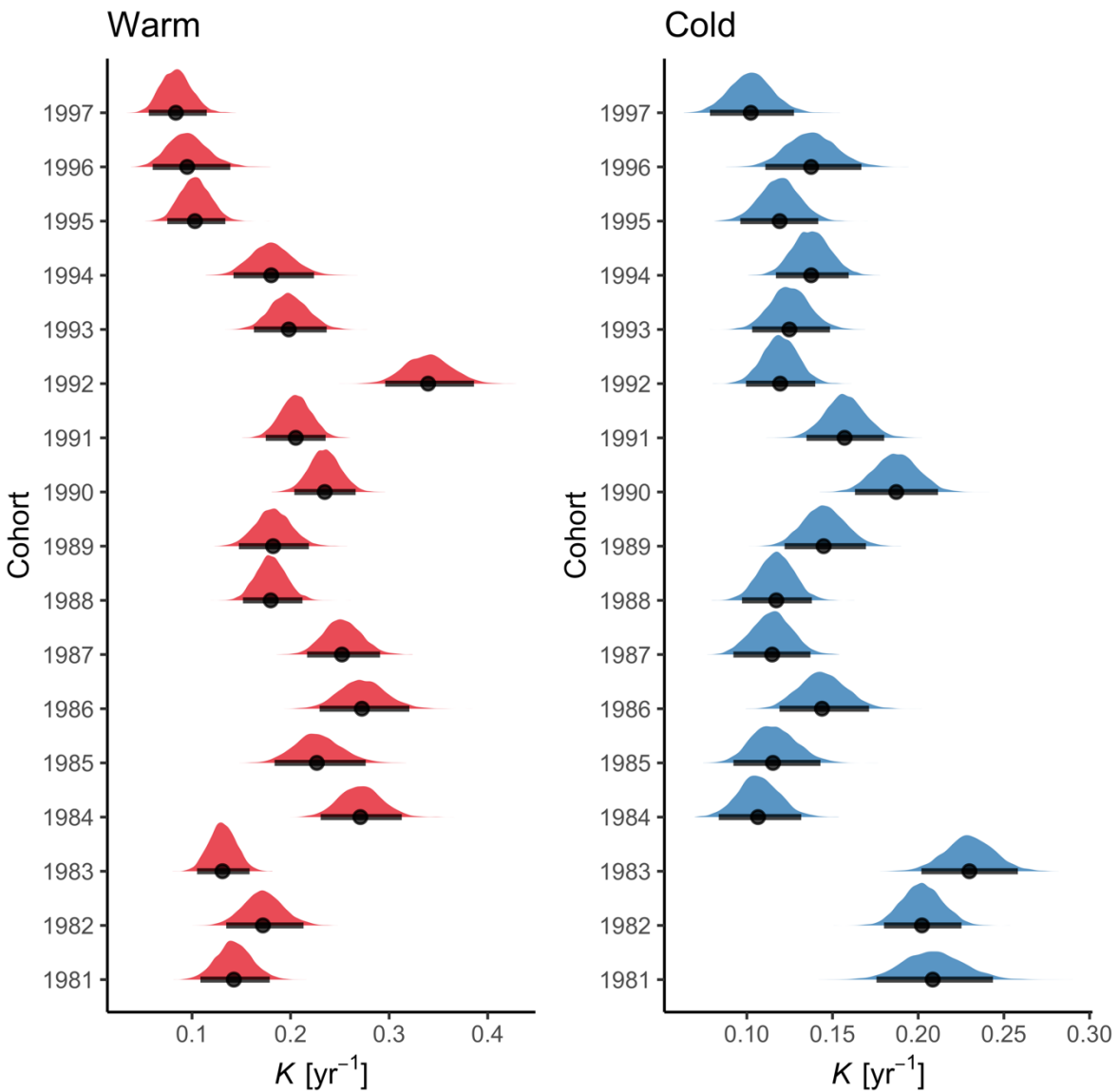


67

68 **Fig. S5.** Posterior distributions of the cohort-varying  $L_{\infty}$  parameter in the best von Bertalanffy  
 69 growth model. Points correspond to the median and the horizontal lines correspond to the 95%  
 70 credible interval. Note that the distributions of  $L_{\infty}$  in the warm areas extend beyond the x-axis  
 71 for cohorts 1995–1997 (also evident in Fig. S3). The range of the x-axis was set to be wide  
 72 enough to include the posterior medians of the larger estimates but narrow enough to allow for  
 73 comparison between the other cohorts and areas.

74

75



76

77 **Fig. S6.** Posterior distributions of the cohort-varying  $K$  parameter in the von Bertalanffy model.

78 Points correspond to the median and the horizontal lines correspond to the 95% credible  
79 interval.

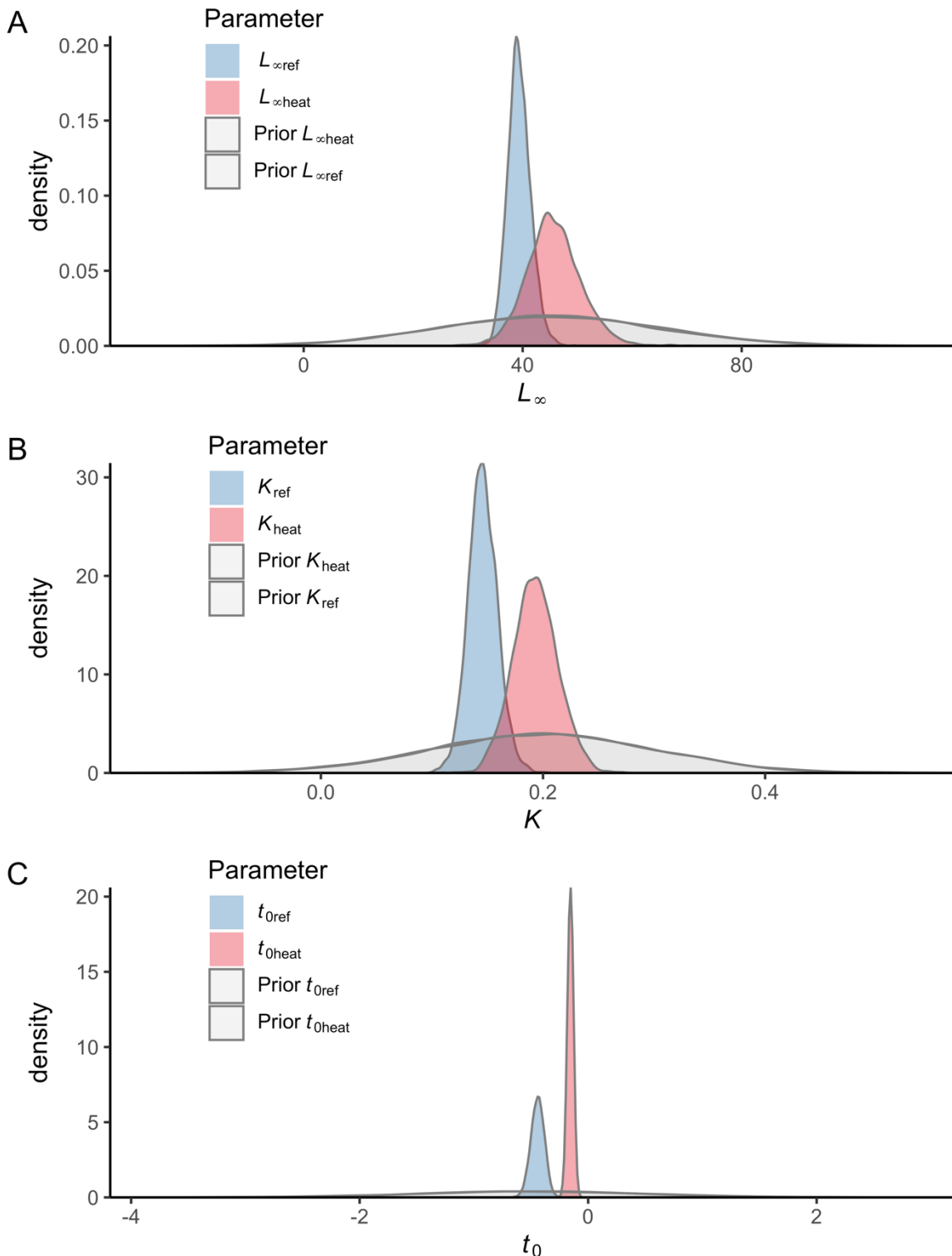
80

81

82

83

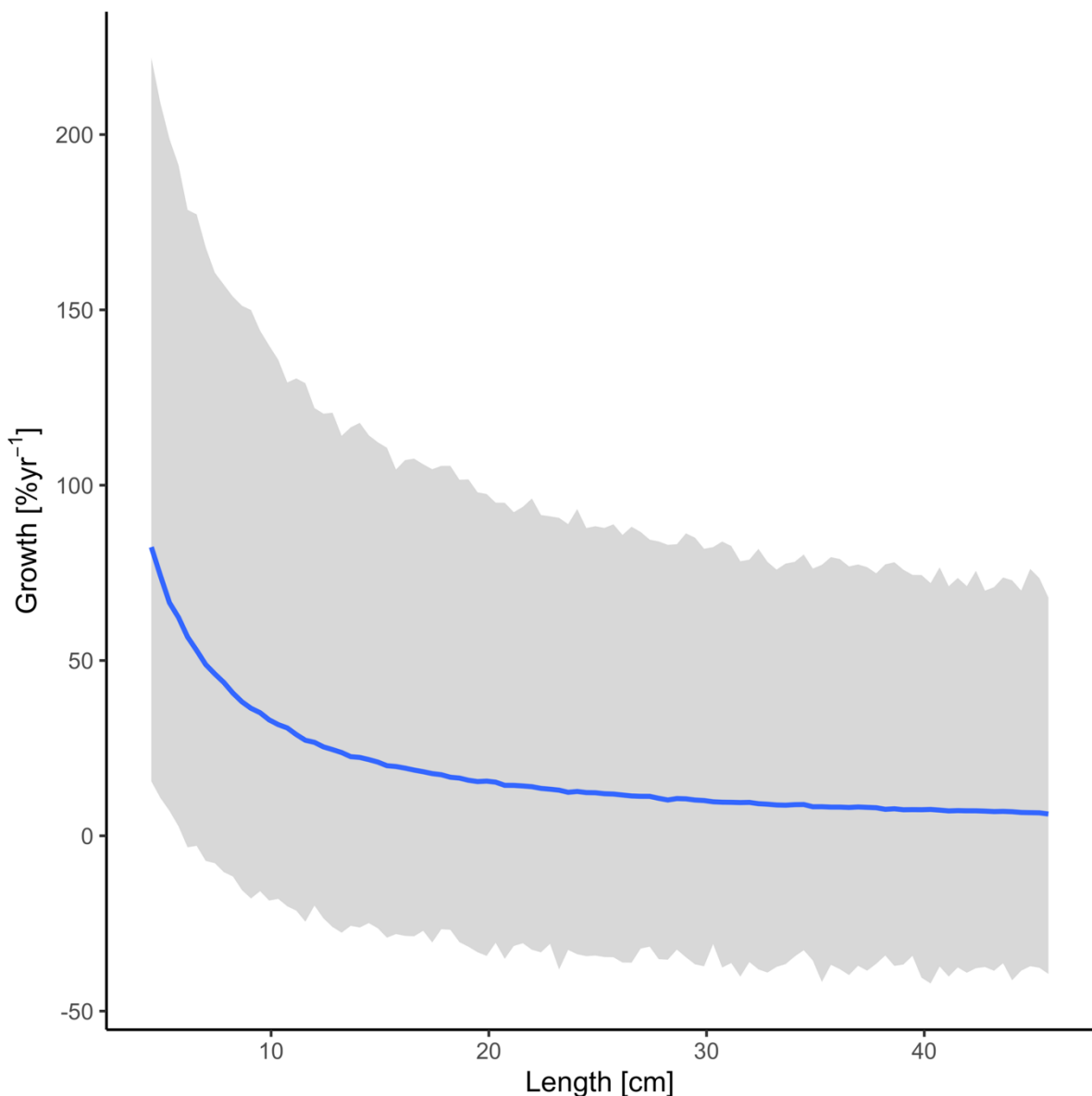
84



85

86 **Fig. S7.** Prior vs posterior distributions for parameters  $L_{\infty}$  (A),  $K$  (B) and  $t_0$  (C) in the best  
87 model of the von Bertalanffy growth equation.

88



89

90 **Fig. S8.** Prior predictive distribution for the allometric growth model (posterior draws from the  
91 prior only, ignoring the likelihood). The solid line is the median and the shaded area is the 95%  
92 credible intervals.

93

94

95

96 **Table S2.** Comparison of allometric growth models with common or unique  $\theta$ -parameter  
97 (exponent in the allometric growth model), ordered by difference in expected log pointwise  
98 density (elpd) from the best model.

Model Name	Model structure	elpd_diff
M1	Intercept ( $\alpha_{j[i],k[i]}$ ) varying across individuals within cohorts, fixed, area-specific slope ( $\theta_{ref}, \theta_{heat}$ )	0
M2	Intercept ( $\alpha_{j[i],k[i]}$ ) varying across individuals within cohorts, “fixed” common slope ( $\theta$ )	-2.7

99

100

101

102

103

104

105

106

107

108

109

110

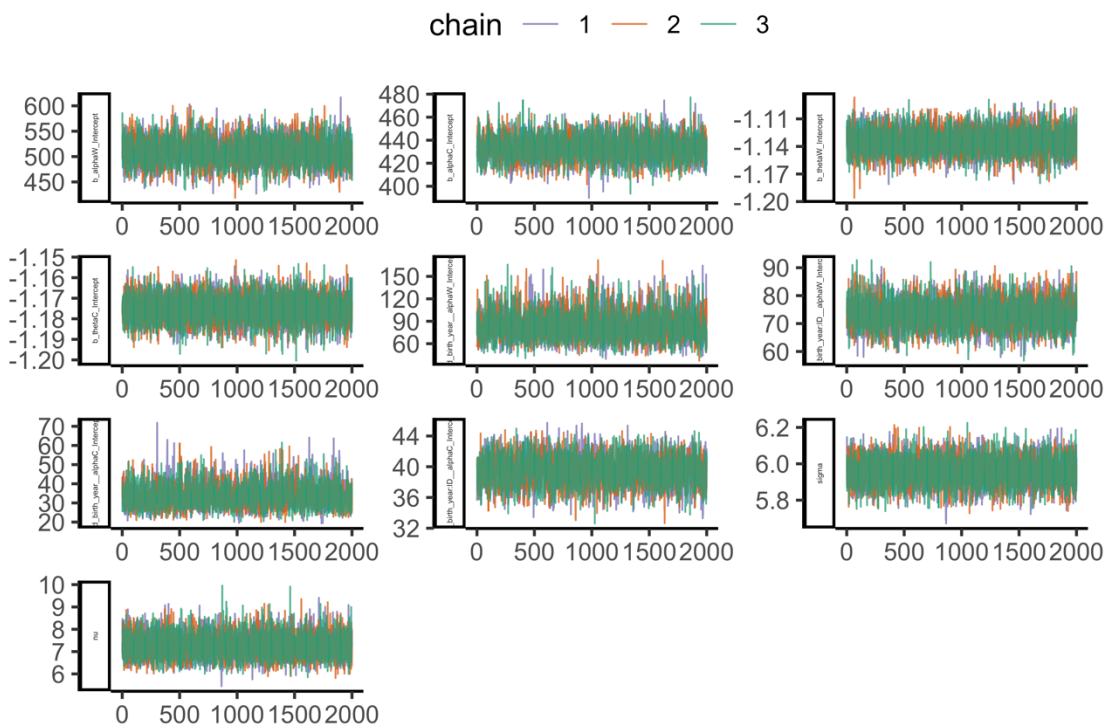
111

112

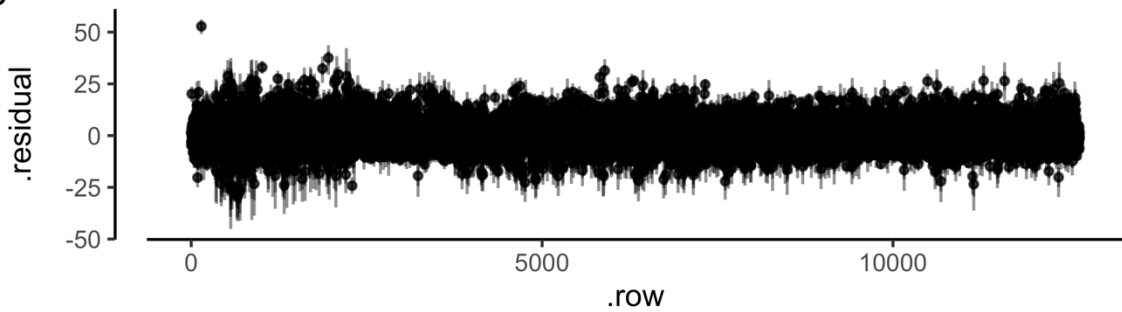
113

114

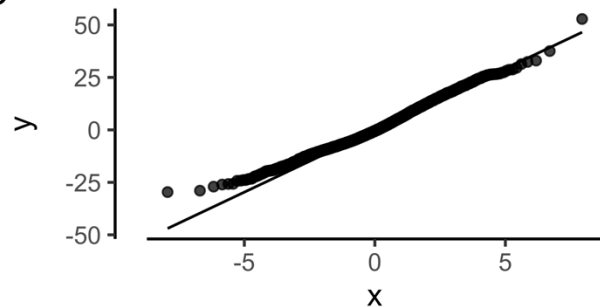
A



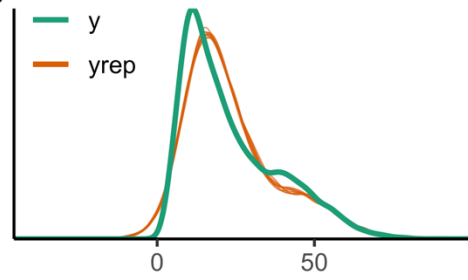
B



C



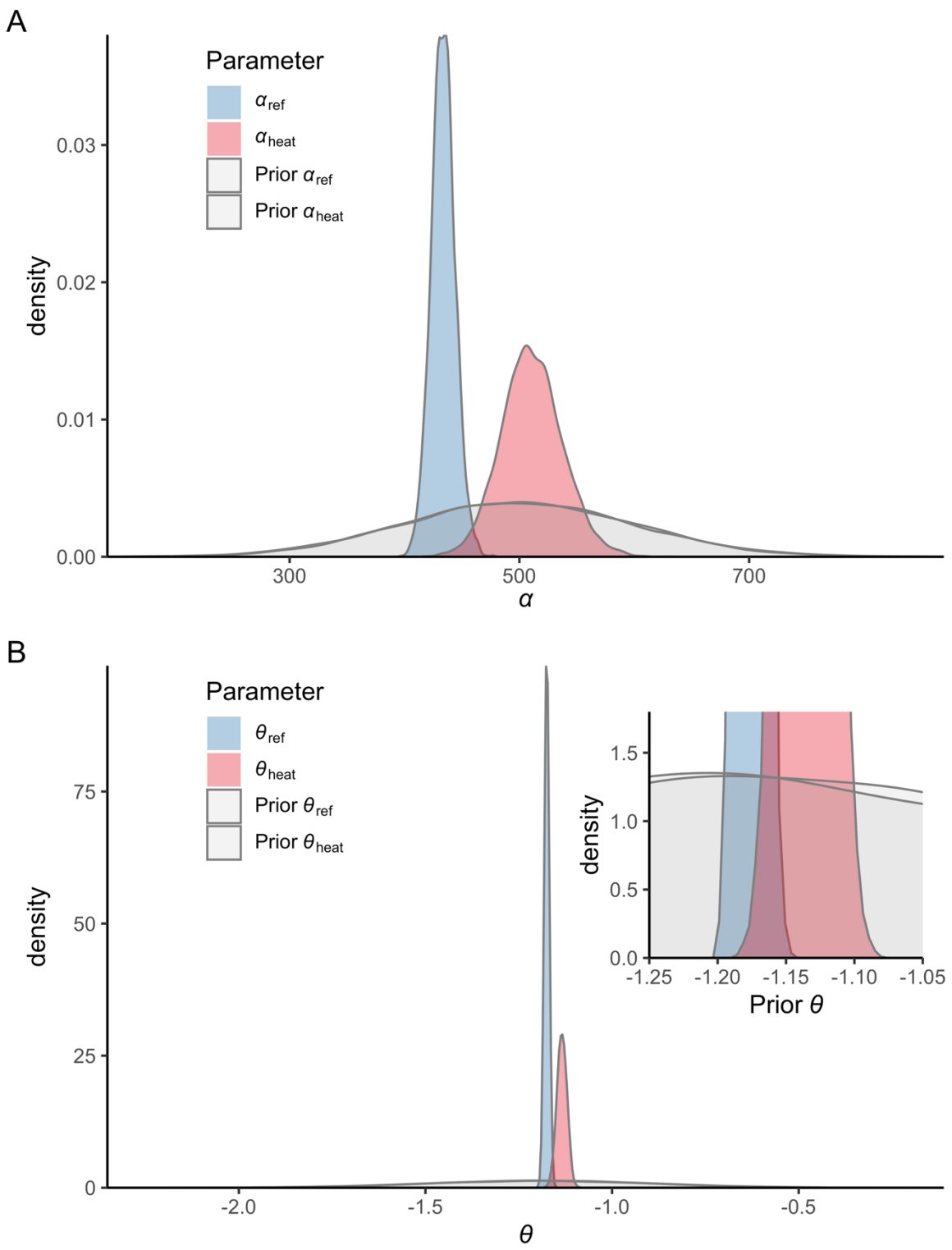
D



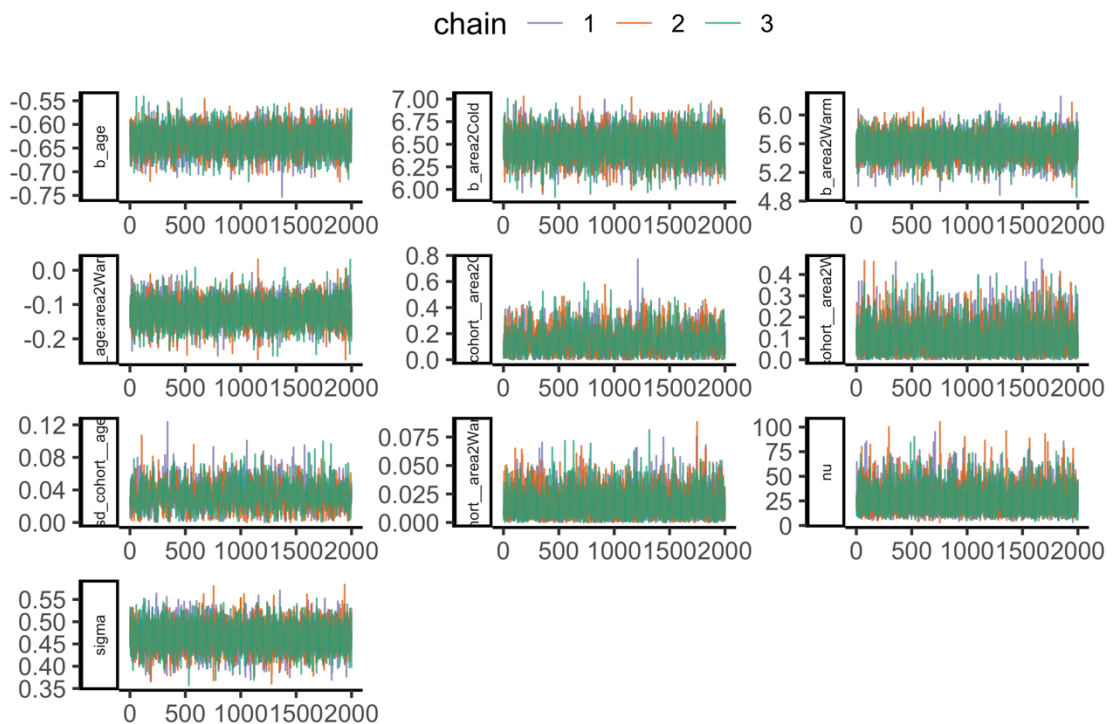
115

116 **Fig. S9.** The best allometric growth model: (A) traceplot to illustrate chain convergence for  
 117 key (population-level) parameters, (B) residuals, (C) QQ-plot and (D) posterior predictive  
 118 check (D).

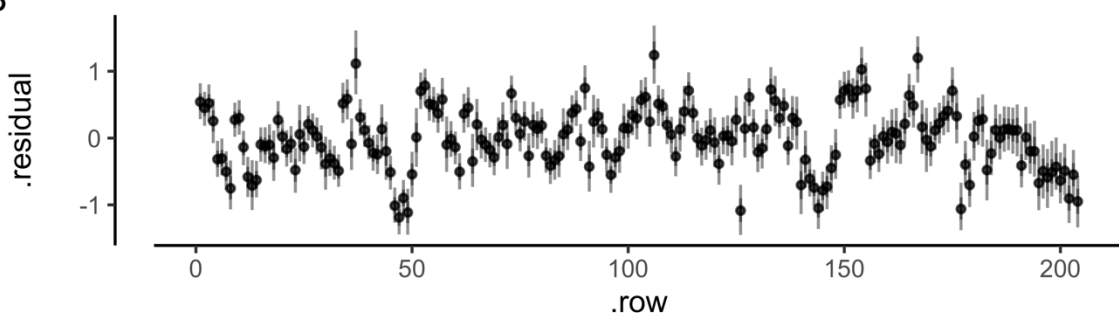
119



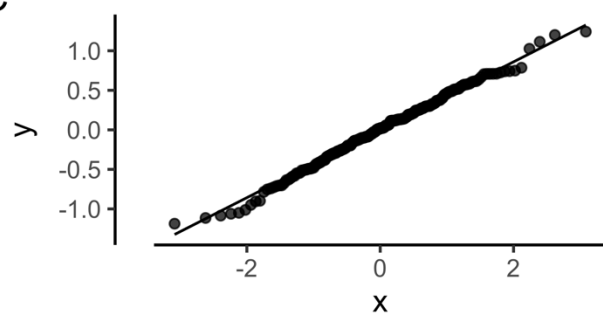
A



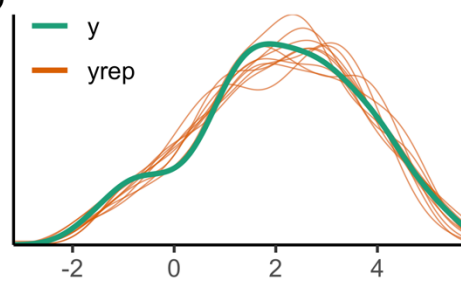
B



C



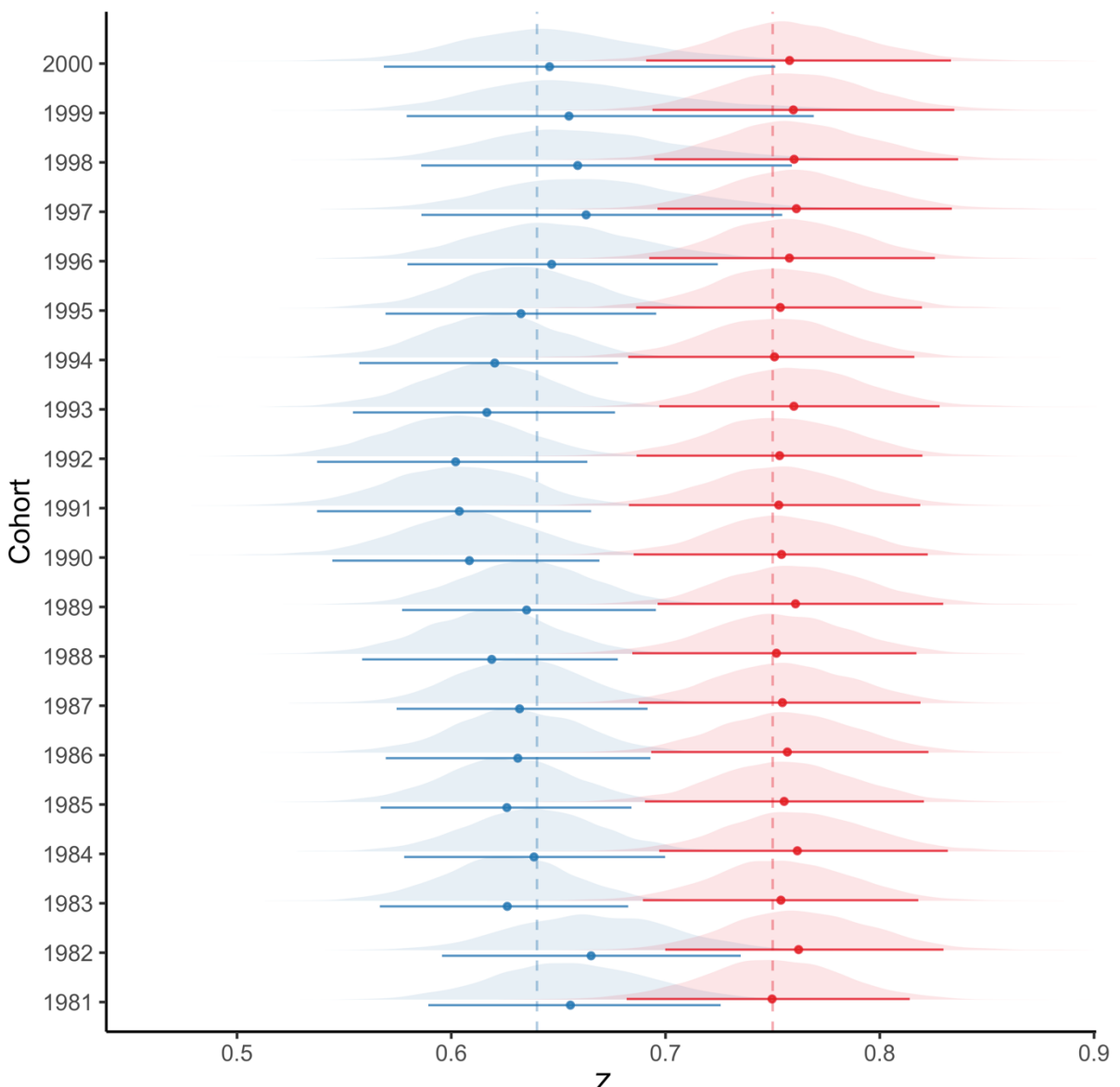
D



125

126 **Fig. S11.** The best catch curve model: (A) traceplot to illustrate chain convergence for key  
 127 (population-level) parameters, (B) residuals, (C) QQ-plot and (D) posterior predictive check  
 128 (D).

129



130

131 **Fig. S12.** Posterior distributions of the cohort-varying slopes in the best catch curve model,  
 132 where  $Z$ , the mortality rate, is the negative of the slope of natural log of catch per unit effort  
 133 (CPUE) as a function of age. Points correspond to the median and the vertical lines correspond  
 134 to the 95% credible interval.

135

136

137

138

139